Behavior of moisture in mortar and concrete after exposed to high temperature

（高温暴露後のモルタル，コンクリート中の水分挙動）

学位取得年月　2019年03月

Daungwilailuk Totsawat

Summary of the dissertation

Behavior of moisture in concrete after exposed to high temperature

(高温暴露後のモルタル，コンクリート中の水分挙動)

Daungwilailuk Totsawat

The aim of this study is using electrical resistivity method to investigate how moisture penetrates into structurally sound, post-fire concrete, by performing experiments on mortar and concrete specimens. The chloride and CO_2 penetrations into post-fire mortar specimens are also investigated in this study to assess the durability of post-fire concrete structures.

Mortar and concrete specimens with water to cement ratio of 0.35 and 0.45 (M035 and M045 for mortar specimens and C035 and C045 for concrete specimens) were prepared in this study. Polypropylene (PP) fibers was also applied to mortar and concrete with W/C of 0.35 (M035PP and C035 PP for mortar and concrete specimen, respectively) at a dosage of 0.2% by volume. After curing in water for 28 days and storing for 30 days, one surface of each specimen was exposed to a temperature of 350°C for 15 minutes. Then, the moisture transfer in the specimens stored at 20°C and 60% relative humidity was assessed by measuring their electrical resistance. The penetration of CO_2 and chloride ions was also examined in the both of specimens. $Ca(OH)_2$ (CH) content in mortar specimen was examined in mortar specimen.

For each W/C of mortar and concrete specimen, compressive strength of heated M035, M045 and M035PP specimens was reduced by 17, 28 and 15%, respectively. On the other hand, high temperature reduced the compressive strength of heated C035, C045 and C035 PP by 25, 18 and 15%, respectively. Micro-cracking inside heated specimen due to pore pressure caused deterioration of compressive strength which increment of porosity of heated specimens is an evidence.

Using the electrical resistivity method, two-point uniaxial technique, it was observed that the electrical resistivity of heated specimen at the depth from exposed surface was higher than that of the inside of specimen. Compared with the unheated specimen, the resistivity at the inside of the heated specimens suddenly decreased. Electrical resistivity and conductivity are reciprocals. Thus, it indicated that the moisture contents of heated specimens at a shallow depth was lower than that of the greater depth. It could be said that the moisture at a shallow depth was evaporated to outside and a part of vapor migrated to greater depth which condensed into moisture. The volume increments of pore of all heated specimen also led to easier transfer of water vapor.

The penetration of CO_2 and chloride ion into the heated mortar and concrete specimens were easier than that in the unheated specimens. The volume increments of pores due to micro-crack and space generation of melting of PP fibers are supposed to accelerate the penetration of heated specimens. Furthermore, the low moisture contents at a shallow of the heated specimen also led to easier penetrate of CO_2 and chloride ion. And the CH was not dehydrated by high temperature in this study.

The moisture at depths close to the exposed surface of mortar, and concrete specimens during the heating is evaporated, and then, a part of vapor migrates to the inside and condenses into moisture inside the specimen. That phenomenon can be observed by the electrical resistivity method. The increase porosity caused by micro-crack and melting of PP fibers leads to easier penetration of CO_2 and chloride ions into the specimen after heating.

Abstract

Daungwilailuk Totsawat

In the case of fire accident, it was found that post-fire concrete structures do not need repairing when they have no spalling and their remaining compressive strength is appropriate for using. Even if it seems not to need repairing, when temperatures in concrete rise highly, chemical compositions and physical structures can be changed, such as dehydration reaction and cracking, resulting in easier ingress of moisture into post-fire concrete.

The aim of the research is to understand how moisture, carbon dioxide (CO_2) and chloride ions penetrate into usable post-fire concrete using electrical resistivity method. The residual calcium hydroxide (CH) is also investigated.

Mortar and concrete specimens with water-to-cement ratios (W/Cs) of 0.35 and 0.45 were prepared for testing. Polypropylene (PP) fiber was applied to the specimens with W/C of 0.35. Five surfaceท of each specimens were covered by insulation materials to ensure that the high temperature could not affect the side of the sides of the specimen. One surface of each specimen was placed on a hot plate and exposed to a temperature of 350°C for 15 minutes with increment of temperature at a rate of approximately 20°C/min. The compressive strength and splitting tensile strength were measured after cooling down of heated specimen. On the other hand, the moisture transfer in the specimens stored at 20°C and 60% relative humidity was immediately assessed by measuring their electrical resistance through a couple of stainless steel rod (two-point uniaxial technique). The penetration of CO_2 and chloride ions was examined in the mortar and concrete specimens. The residual CH was investigated to ensure that the CH was not dehydrated by high temperature and did not produce calcium oxide (CaO), which it can affects carbonation.

After heating, the pore volume of heated mortar specimens was increased due to micro-cracking and melting of PP fiber, which the cracking and melting of PP fiber could be observed in SEM images. The micro-cracking also reduces the residual compressive strength of heated mortar and concrete specimens. The residual compressive strengths of heated mortar and concrete specimens are higher than 70% and 75% of unheated specimen, respectively.

By using two-point uniaxial technique, the electrical resistance of surface regions of the specimens was greater than at greater depths and the unheated specimens had the lowest resistance. It could imply that these regions of the heated specimens with and without PP fibers are drier than those of unheated specimens. It is due to evaporation and migration of moisture under high temperature. The increment of pore water vapor due to vapor migration into inside the mortar and concrete specimen create micro-cracking. The heated mortar specimens exhibited greater penetration of CO_2 and chloride ions compared to the unheated specimens. It could be said that the increment of pore volume and low moisture content in the heated specimen can accelerate carbonation and chloride penetration. PP fibers and high W/C also increased the rate of carbonation and chloride penetration into the mortar and concrete specimens after heating.

Contents

Figures and tables contents

1. Introduction

1.1 Background

Concrete is one of the most favorite material in modern construct work. Nowadays, there are several types of concrete that are used in the world, high strength concrete, compaction concrete and chemical resistance concrete and etc. However, whatever, concrete have been degraded by several factors such as environment (i.e. freeze-thaw, sulfate in seawater and acid rain etc.), accident and its quality such as low-skill labor, impurity of material etc. In the case of environmental, although, carbon dioxide (CO_2), chloride and sulfate are causing of deterioration, it still takes many years to corrodes reinforcing steel bar or crack on concrete. But an accident can be occurred in any time and immediately cause the damage on concrete. Fire accident is a scenario that concrete structure can be exposed to at any time. The loss in compressive strength, modulus of elasticity, chemical bonding or cracking is immediately occurred after fire accident. Behavior of concrete under fire condition has been known since the last century and studied by many researchers (Papayianni and Valiasis, 1991, Lin et al., 1996, Chan et al., 1999)

Nowadays, several assessment techniques have been used to determine the condition of concrete and the changes to the physical properties of material after exposure to fire such as a Schmidt Rebound Hammer, Differential Thermal Analysis (DTA), Thermal Gravimetric Analysis (TGA), micro-crack density analysis, image analysis, etc (Annerel and Taerwe, 2013). However, these tests can be divided into two types, in situ techniques and laboratory tests. The situ techniques include Destructive Testing (DT), coring test, Non-Destructive Testing (NDT) and Ultrasonic Pulse Velocity (UPV).

However, less attention has been paid to post-fire durability of fire exposed concrete structures where the mechanical properties are not considerably influenced. The durability of concrete is governed by the transport properties under the presence of moisture, CO_2 and chloride. Post-fire concrete at this state may or may not need repairs. In the case of required repairing, the cost of fire damage restoration will be determined by the condition of post-fire concrete. But the investigation method on post-fire concrete is limited by the unknowable damage of concrete.

1.2 Objectives and limitations

The aim of this study is to investigate how moisture penetrates into structurally sound post-fire concrete, using electrical resistivity method by performing experiments on mortar and concrete specimens. In this study, the high temperature, 350˚C at the surface of specimen, is applied in the experiment instead of fire in order to degrade some mechanical properties and avoid changing of Calcium Hydroxide (CH) content. The chloride and CO_2 penetrations into post-fire mortar specimens are also investigated in this study to assess the durability of post-fire concrete structures. This study focuses on mortar and concrete exposed to high temperature.

2. Literature reviews

This chapter discusses, the literature study on fire mechanism, properties and mechanism of concrete under fire, moisture role in concrete under fire, the relation between electrical resistance and moisture inside the concrete and benefit of polypropylene fibers (PP fibers). The motivation of the study is also presented in this chapter.

2.1 Fire

Three elements must be present simultaneously: oxygen, combustible material and a heat source to ignite. The different phases in the development of a fire are shown in Fig. 1. It shows the evolution of the temperature in the compartment as a function of time.

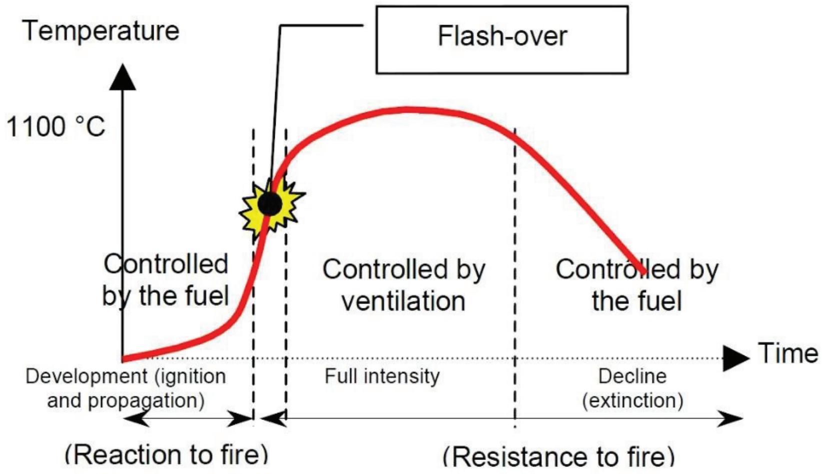

Fig. 1 Temperature development stages in a real fire (Denoël 2007)

A heat source causes a fire to start in a quantity of materials (fuel). In a closed environment, if the oxygen is sufficient for combustion, the fire will be controlled by fuel. During the development of fire, the temperature is so high that it causes any combustible element in the compartment to ignite. This phenomenon is called flash-over. The heating rate is accelerated during flash-over which could be life threatening (FIB 2007). Then, the fire is growing up to be fully developed. The oxygen at this phase is insufficient for combustion. Thus, the fire will be controlled by ventilation. After that, when more or less 70% of the fuel has been consumed, the temperature drops as seen in the final phase.

The response of concrete to fire depends upon the nature of the fire which can vary considerably. The key feature of the fire relevant to the concrete structure is the temperature-time curve imposed by the fire at its surface. The key parameters of those are as follow:

A) The heating rate which influences the development of temperature, moisture and pore pressure gradients within the concrete structure

B) The maximum temperature which influences the nature of the physical-chemical relations in the material and its properties

C) The duration of the fire which influences the temperature development in the structure with time.

D) The cooling regime, water cooling would have a different influence upon the material and the temperature distribution from natural cooling.

The simply way of representing a fire exposure is to use standard fire curves that is giving the evolution of the temperature of the gases as a function of time. The standard fire curves were developed to test structural elements experimentally. The curves most frequently used are Hydrocarbons curve, Hydrocarbon modified curve, ISO 834 curve and ASTM E119 curve, as seen in Fig. 2 and equation 1-4.

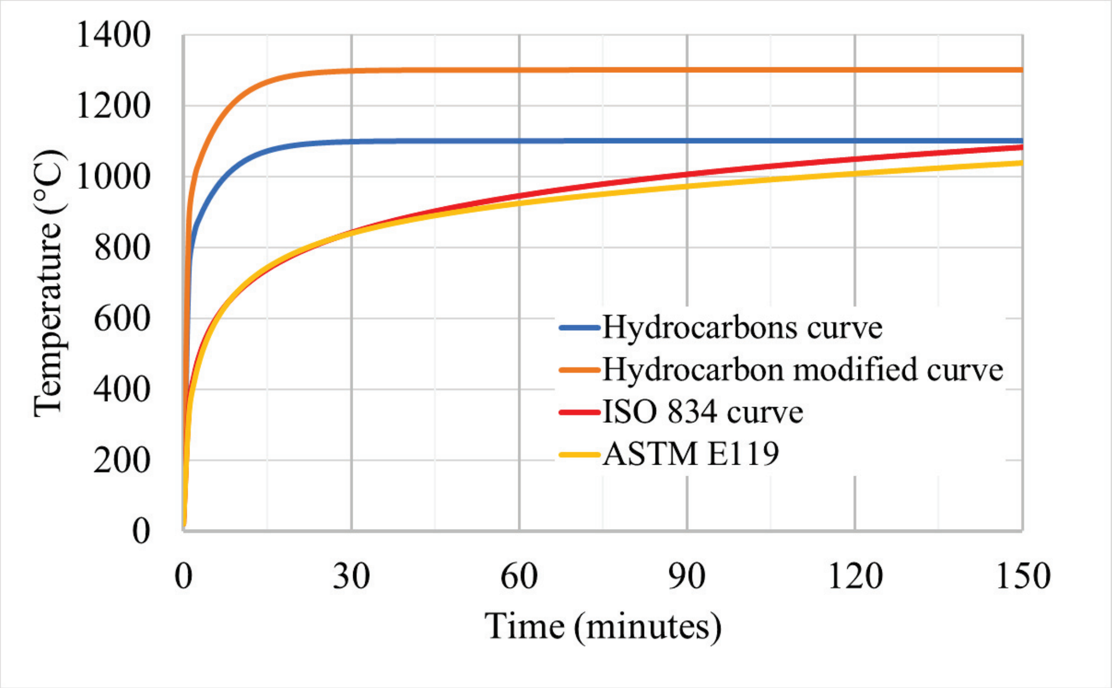

Fig. 2 Standard fire curves

Hydrocarbons curve

$$T = T_0 + \left(1080 \times \left(1 - (0.325e^{-0.167t}) - (0.675e^{-2.5t})\right)\right) \quad (1)$$

Hydrocarbon modified curve

$$T = T_0 + \left(1280 \times \left(1 - (0.325e^{-0.167t}) - (0.675e^{-2.5t})\right)\right) \quad (2)$$

ISO 834 curve

$$T = T_0 + 345\log(8t + 1) \quad (3)$$

ASTM E119

$$T = T_0 + \left(1 - e^{-3.79553\sqrt{t}}\right) + 170.41\sqrt{t} \quad (4)$$

2.1.1. Fire severity

Fire severity is not a standardized term. It is, however, generally accepted that is represent the detrimental effect of a fire on the concrete structure elements. There are a number of methods which, utilizing various input parameters, convert the calculated intensity of a fire, expressed by various means, to the equal duration of exposure in a test furnace under one of the standardized time-temperature conditions.

In summary, the severity of the fire is characterized by the following factor: A) the duration of the fire, B) the average temperature in the compartment and C) the speed with which the fire developed and with which the temperature rise (Wade et al.,2014, Denoël 2007)

2.2 The response of concrete to high temperature

2.2.1. The characteristic of concrete

Generally, when exposed to high temperature lower than 100°C, concrete is still sound. When concrete is exposed to 300°C, the color of concrete is changed to red/pink due to oxidation of ferric salts in aggregates (concrete society 2008) and its compressive strength is reduced by about 15%–40% because tiny cracks appear along the boundaries of calcium hydroxide (CH) crystals (Georgali and Tsakiridis 2005). For CH dehydration, the actual temperature at which CH dehydrates is not established. Several literatures have reported that it is in the range of 350 - 550°C (Lin et al. 1996; Georgali and Tsakiridis 2005; Omer 2007; Rongviriyapanich et al. 2016). At 550°C, the compressive strength is reduced by approximately 55-70% and aggregates begin to deteriorate. Quartz in siliceous aggregates polymorphically changes with a volumetric expansion and consequent damage (Georgali and Tsakiridis 2005; concrete society 2008). Large cracks appear within cement paste and around aggregate particles when concrete is exposed to 600°C. At this temperature, the color of concrete begins to change to white/gray due to calcination of calcareous components in cement matrix and fine aggregate (concrete society 2008). When concrete is exposed to 1,000°C, cracks become extensive but at 1,200°C, the concrete completely decomposes and lost its binding properties due to excessive cracking, spalling and explosion (Lin et al. 1996; Omer 2007; Kalifa et al. 2001). The degradation of concrete is shown in Fig. 3 (Omer 2007)

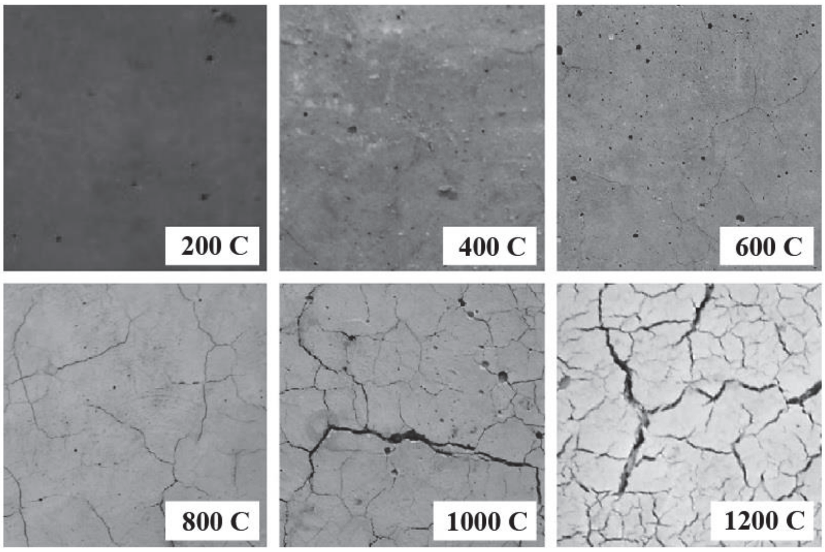

Fig. 3 Surface of concrete exposed to elevated temperatures (Omer 2007)

2.2.2. The compressive strength and modulus of elasticity

As mentioned in previous section, there are physical and chemical changes in cement paste and aggregates. Many factors affecting the concrete damage level are as follow: heating rate, maximum temperature, duration of exposure to temperature, moisture content of the concrete, etc. The residual compressive strength of post-fire concrete depends on the exposed temperature. However, fib (2007, 2008) and Kodur (2014) reported that the various factors of concrete have significantly affected the degradation of compressive strength such as type of aggregate, concrete age and the type of cement. Fig. 4 shows the compressive strength of concrete at elevated temperature which is reported in Eurocode (2004). It diminishes with respect to an increment of temperature in both siliceous and calcareous aggregates. During fire, thermal incompatibility between the aggregate and cement paste cause parasitic thermal stress inside, resulting in micro-cracking and reducing compressive strength as seen in Fig. 5 and Fig. 6. Furthermore, in the case of the normal strength concrete (NSC), it is usually highly permeable and allows easy diffusion of pore pressure caused by water vapor. On the other hand, high strength concrete (HSC) produces a dense microstructure, the use of binders such as slag and silica fume can improve the compressive strength at room temperature, durability also, resulting in dense microstructure, which attributes to high impermeability and enhances pore pressure. Finally, the built-up pore pressure results in rapid development of the micro-crack resulting in deterioration of the compressive strength. Rongviriyapanich et al. (2016) reported that the flexural strength of mortar specimens was slightly increased compared with the compressive strength in the early stage of burning. After that it was rapidly decreased in the greater burning time due to the existence of cracks induced by fire.

Additionally, the lower value of the compressive strength is also attributed to supplementary damage due to additional stresses caused by cooling. The extent of stresses depends on the rate of cooling. Therefore, rapid cooling or quenching results in higher levels of damage (Hanger, I. 2013). Consequently, the modulus of elasticity of concrete decreases with the increment of temperature regardless of water to cement ratio (W/C).

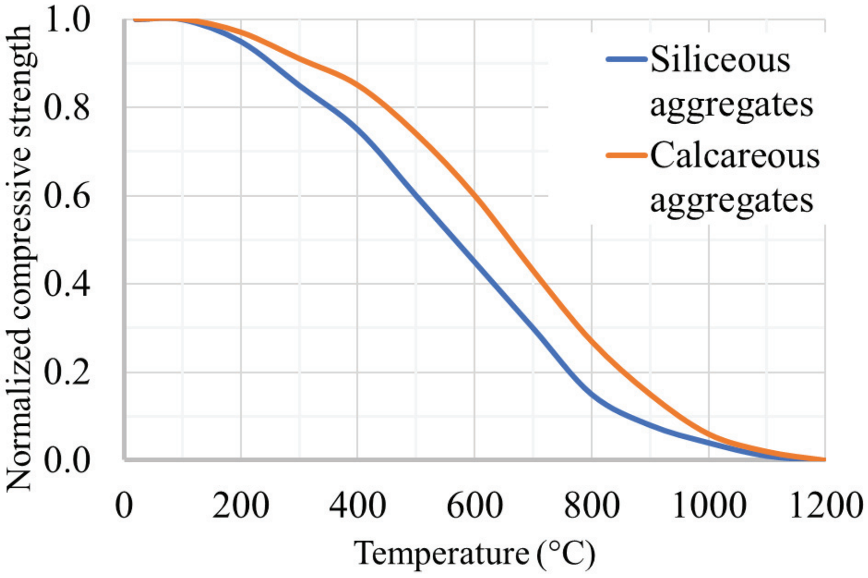

Fig. 4 Variation of compressive strength at elevated temperature by Eurocode

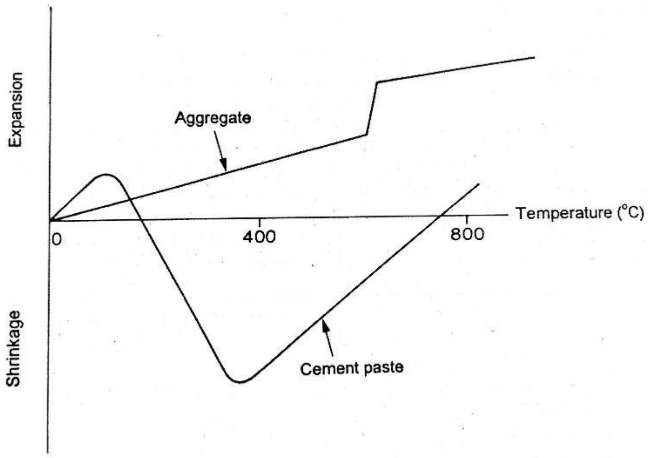

Fig. 5 Thermal incompatibility of the aggregate and cement paste causing parasitic thermal stress

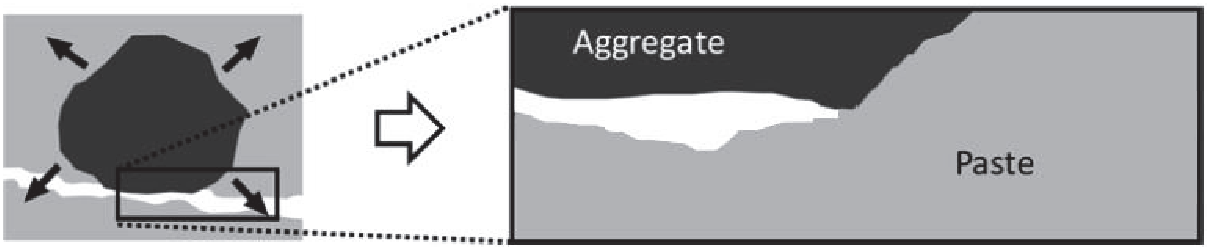

Fig. 6 Micro-cracking due to thermal incompatibility of coarse aggregate and cement paste

2.3 The response of moisture content to concrete

Concrete is porous material that contains water and moisture inside. Several mechanical properties are influenced by the moisture content because of the interaction of solid matrix and pore water, such as the rate of reinforcement corrosion, freeze thaw attack, carbonation reaction, high temperature spalling, etc. Therefore, it can be said that water/moisture penetration and water/moisture content as well as high temperature is one of the factors related to the degradation and deterioration of concrete, which the penetration is permitted by the microstructure of any concrete. The main transport of water/moisture occur through the continuous phase of the cement paste. The higher transport properties are found in the porous zone between the aggregate and the cement paste which it is called the interfacial transition zone (ITZ). Nevertheless, the contribution to the total transport is depended on continuity of ITZ. Additionally, the moisture condition inside the concrete even influences transport of gases and ions. In the other words, reducing the moisture transport in concrete will considerably improve the durability.

Yufang and Lianchong (2011), Ozawa and Morimoto (2014) and Lu (2015) reported that the migration of moisture and water in concrete during heating is in the porous network of concrete, where water vapor not only evacuates to the heated surface and evaporates to atmosphere, but they also migrate to the inside of concrete, which is a cooler region. Nearest the heated surface there is a dry zone, thickness of which increases with exposure time. The vapor that migrated inward is cooled down and condenses to water. It means that the moisture content at inside the concrete is increased. This process continues during heating, despite the inside being saturate, which causes less vapor transport towards the inside. The moisture clog generates high pressured, resulting in micro-cracking, spalling and explosion.

Generally, the permeability of post-fire concrete has been rapidly increased on high and moderate fire exposed (Kalifa et al. 2001; Noumowe et al. 2009; Joakim 2015). This results in easier penetration of moisture and gas into post-fire concrete (Poon et al. 2001, 2003). However, less attention has been paid to moisture transfer of post-fire concrete structures where the mechanical properties and chemical properties are not considerably influenced.

2.4 The response of electrical resistivity to moisture content

As a method for measuring the water content inside concrete, gravimetric determination has been used but concrete must be cut to measure its mass. The destruction of the concrete is a disadvantage of this method, even though it is a reliable method. Furthermore, a lot of specimens are required to know the changes in the mass over time. The electrical conductivity of a concrete material is capability of concrete to transfer ions, which, the electrical resistivity is the invert of electrical resistance. Generally, several electrolytic, such as K^+, Na^+, SO^- and OH^-, contain in pore water. Therefore, electrical resistivity in concrete is expected to be a function of the degree of water saturation of concrete. The electrical resistivity of wet concrete is in the range of $10^5 \Omega \cdot mm$, while dry concrete has resistivity in the range $10^{12} \Omega \cdot mm$. The variation of electrical resistivity in wet and dry concrete can be interpreted as meaning that the electrical resistance has been significantly affected by evaporated water (Madhavi and Annamalai 2016). Electrical measurement (resistivity and conductivity) is an alternative method to monitor the moisture of concrete in place and is a non-destructive method (Mccarter et al. 1995, 2001; Rajabipour et al. 2004). Additionally, the electrical resistivity method is more economical because a few of specimens are required. The electrical resistivity method has been carried out to monitor moisture content at specific time and specific position in a mortar specimen by several researchers. But the information of the method on post-fire concrete has been scarce in literature. A non-destructive measurement method which can be applied in place is necessary to assess the damage of post-fire concrete. Therefore, in the present study, the electrical resistivity method is used to investigate moisture content inside the mortar and concrete specimens after exposed to high temperature.

Elkey and Sellevold (1995), Layssi et al. (2015) and Madhavi and Annamalai (2016) have reported that the current flow in concrete is due to the ionic movement within the pore structure, and ionic movement is affected by temperature. An increase in the temperature increases ionic movement, which turns to decreases the electrical resistivity (electrical resistance). It has been reported that the temperature change in 1°C at 21°C can result in 3% change in electrical resistivity of concrete at saturated surface dry condition and result in 5% change in electrical resistivity of concrete under 30% saturation, with resistance increasing with decreasing temperature (Elkey and Sellevold 1995; Layssi et al. 2015). The effects of temperature, internal moisture content and pore structure are also discussed in this paper.

2.5 The response of Polypropylene fibers (PP fibers) to high temperature

Generally, 1-2 kg/m^3 of PP fibers are used in the concrete mix to reduce the fire spalling of concrete, although amounts both below and above this range are sometimes used. This amount corresponds to 0.4-0.8% of the cement paste volume assuming that the cement paste occupies 30% of the volume of concrete. The most common type of PP fibers starts to melt at approximately 160°C and the degradation reaction is completed at approximately 380°C according to Schneider and Horvath (2003). However, some researcher reported that melting point of PP fibers is 150°C and the temperature at approximately 176°C is complete melting (Khoury and Willoughby 2008).

After melting of PP fibers, capillary pores are created leading to an improved permeability of concrete. Schneider and Horvath (2003) claim that the fibers must gasify before free space of pores are created, while Kalifa et al. (2001) conducted an experiment to show that PP fibers can be absorbed by cement matrix during heating. However, the concept that PP fibers can be absorbed into the cement matrix has been criticized by Khoury and Willoughby (2008) because of the high viscosity of the PP fiber melt which will limit this absorption whereas Richardson and Dave (2008) supported the concept of absorption of melted PP fibers into the cement matrix.

2.6 Motivation of work

The most of research in the past paid attention to chemical and physical properties of concrete during and after fire. But less attention has been paid to durability of post-fire concrete where the mechanical properties and chemical properties are not considerably influenced. At this level, the post-fire concrete may not appear to need repairs as mentioned in this chapter, but some of its chemical and physical properties could have changed, due to dehydration reactions, degradations of modulus of elasticity, etc. Consequently, those concrete structures exposed to high temperatures have a risk of deterioration due to changes in mechanical properties and mineral compositions. Moisture is one of main factors causing the degradation and deterioration of concrete structure. Thus, the reliability information of moisture in usable post-fire concrete is important to observe. However, the appropriate method should be applied. Thus, the electrical resistivity method which is an in situ and nondestructive method is chosen. In addition, post-fire concrete is easy for chloride ions and carbon dioxide to penetrate into concrete after exposure to high temperatures. A study of the diffusion of these two species is also necessary to indicate the durability of concrete.

3. Methodology

In this experimental work different standardized and non-standardized test methods were used to evaluate residual concrete properties after exposed to high temperature. The parameters varied are concrete mix proportion and time.

3.1 Materials and mixture proportions

In this study, ordinary Portland cement and crushed sand were used as cement (C) and fine aggregate (S), respectively, to make mortar. The fine aggregate used in this study is quartz porphyry. Superplasticizer (SP) and air-entraining admixture (AE) were used to achieve the target air content of 4.5 ± 1.5% and appropriate workability for casting. Mortar specimens with water-to-cement ratios (W/Cs) of 0.35 and 0.45 were prepared. Polypropylene (PP) fiber was applied to the mortar specimen with W/C of 0.35 at a dosage of 0.34% by volume of mortar. This dosage approximately corresponds to 0.2% by volume of concrete, which is generally adopted from the industrial point of view (Behnood and Ghandehari 2009). The characteristics of the PP fibers used in this study are shown in Table 1. The target compressive strength of mortar specimens at the age of 28 days was above 60 MPa to get a fire resistant concrete. The mixture proportions of mortar specimens are shown in Table 2.

For concrete specimens, crushed stone (G) was prepared as coarse aggregate in addition to the above materials. The coarse aggregate used in this study is quartz porphyry. The targets of air content and slump were 4.5 ± 1.5% and 14±2 cm, respectively. The target compressive strength of concrete specimens at the age of 28 days was above 60 MPa. The mixture proportions of the concrete specimens are shown in Table 3. The measured properties of fresh mortar and concrete are shown in Table 4.

Table 1 PP fiber characteristics

Density (g/cm^3)	Diameter (μm)	Length (mm)
0.91	48	20

Table 2 Mixture proportions for mortar specimens

Name	W/C	kg/m^3				Percentage of cement by mass	
		W	C	S	PP	AE	SP
M035	0.35	289	835	1,117	-	0.001	0.5
M045	0.45	289	654	1,270	-	0.001	0.5
M035PP	0.35	289	835	1,117	3.13	0.001	0.5

W: water

Table 3 Mixture proportions for concrete specimens

Name	W/C	kg/m^3					Percentage of cement by mass	
		W	C	S	G	PP	AE	SP
C035	0.35	170	486	651	978	-	0.001	1.5
C045	0.45	170	378	738	980	-	0.001	0.5
C035PP	0.35	170	486	651	978	1.82	0.001	1.0

Table 4 Designed and measured properties of fresh mortar and concrete

Name	Designed		Measured		
	Slump (cm)	Air content (%)	Slump (cm)	Air content (%)	Temperature (°C)
M035	-	4.5 ± 1.5	-	4.5	21.5
M045	-	4.5 ± 1.5	-	4.5	22.6
M035PP	-	4.5 ± 1.5	-	5.0	22.8
C035	14 ± 2	4.5 ± 1.5	16.0	4.5	18.1
C045	14 ± 2	4.5 ± 1.5	12.0	5.0	19.2
C035PP	14 ± 2	4.5 ± 1.5	16.0	4.5	21.3

3.2 Preparation of specimens

3.2.1. Mortar specimen

Mortar was mixed in a mortar mixer, and was casted and compacted in cylindrical and prismatic molds. Mortar specimens of 50-mm diameter and 100-mm height were prepared for compressive strength testing. For temperature monitoring, thermocouples were inserted at intervals of 20 mm in the prismatic specimens of 40-mm width, 40-mm height and 160-mm length, as shown in Fig. 7. For comparison of the internal temperature between the mortar and concrete specimens, the thermocouples were inserted at the same intervals. An interval of 20 mm was selected to limit the effect of aggregates on temperature monitoring because the maximum size of coarse aggregate used in this study was 20 mm. In addition, to measure the temperature near the exposed surface, the first thermocouple was inserted at a depth of 2.5 mm from the exposed surface. The embedded thermocouples were placed approximately 20 mm from the bottom of the specimens.

For moisture transfer examination, stainless steel rods of 0.9 mm in diameter were arranged at intervals of 15 mm in the prismatic specimen of 40 mm width, 40 mm height, and 160 mm length, as shown in Fig. 8. To limit the effect of fine aggregates on the measurement of electrical resistance, an interval of 15 mm, which is three times as large as the maximum size of fine aggregate, was set up. Prismatic specimens of 80 mm width, 40 mm height, and 160 mm length were prepared for carbonation examination, as seen in Fig. 9, and the prismatic specimens of 40 mm width, 40 mm height, and 160 mm length were prepared for chloride penetration examination.

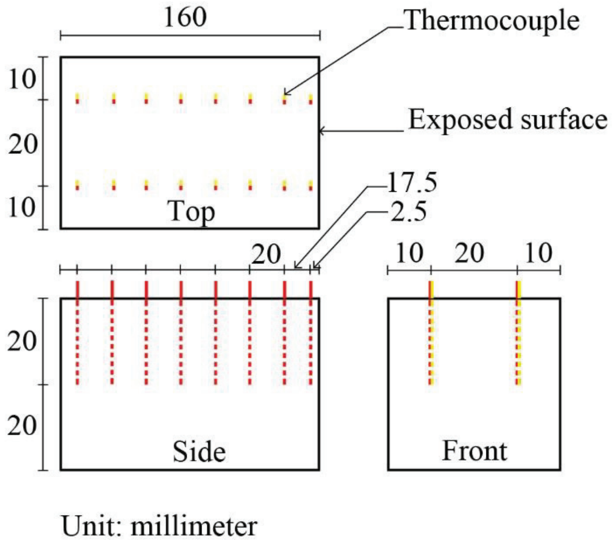

Fig. 7. Mortar specimen configuration for temperature monitoring

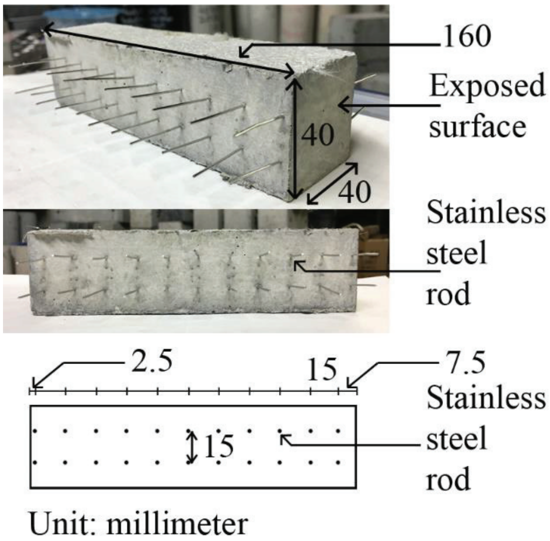

Fig. 8. Mortar specimen configuration for moisture transfer examination

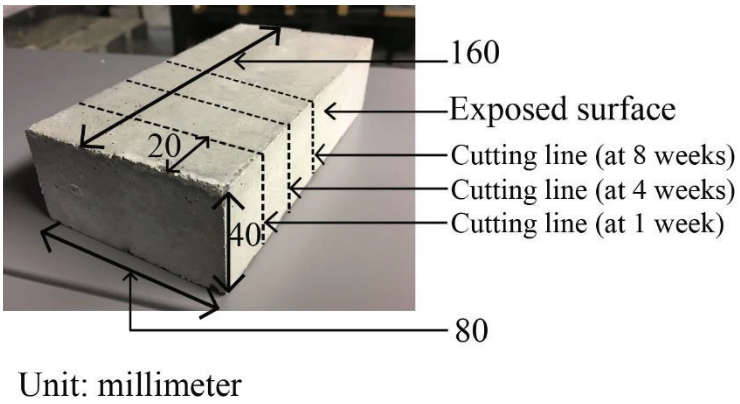

Fig. 9. Mortar specimen configuration for accelerated carbonation test

3.2.2. Concrete specimen

Concrete was mixed in a concrete mixer, and was casted and compacted in cylindrical and prismatic molds. Concrete specimens of 100 mm diameter and 200 mm height were prepared for compressive strength tests. The temperature was monitored by thermocouples which were inserted at intervals of 20 mm in the prismatic specimens of 100 mm width, 100 mm height and 150 mm length, as shown in Fig. 10. Similar to the mortar specimens, the first thermocouple was inserted at the depth of 2.5 mm from the exposed surface to measure the temperature at the depth near the exposed surface. The depth of the embedded thermocouples was approximately 50 mm from the bottom of the specimens.

For the moisture transfer examination, stainless steel rods of 0.9 mm diameter were arranged at a horizontal interval of 20 mm and a vertical interval of 60 mm in the prismatic specimen of 100 mm width, 100 mm height and 150 mm length, as shown in Fig. 11. Similarly to the mortar specimen, an interval of the stainless steel rod of 20 mm was selected to limit the effect of coarse aggregates on measurement of the electrical resistance.

In this study, the carbonation examination was also conducted. The prismatic specimen of 100-mm width, 150-mm height and 400-mm length was prepared for carbonation examination, as seen in Fig. 12. Meanwhile, the prismatic specimens of 100 mm width, 100 mm height, and 150 mm length were prepared for chloride penetration examination.

All of mortar and concrete specimen of each tested were summarized and shown in Table 5.

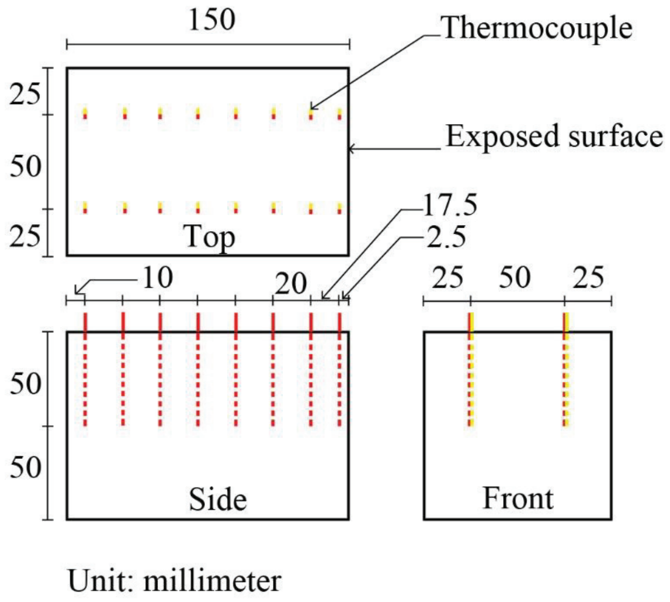

Fig. 10 Concrete specimen configuration for temperature monitoring

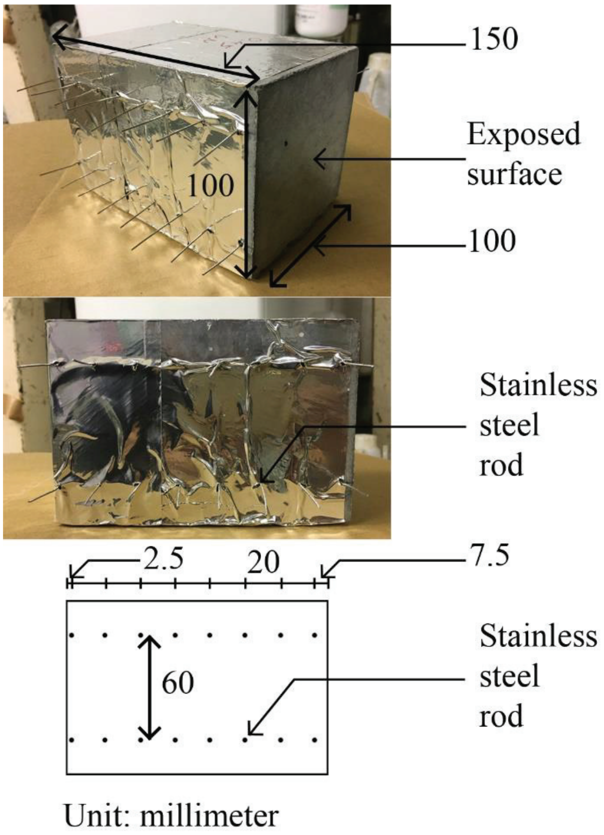

Fig. 11 Concrete specimen configuration for moisture transfer examination

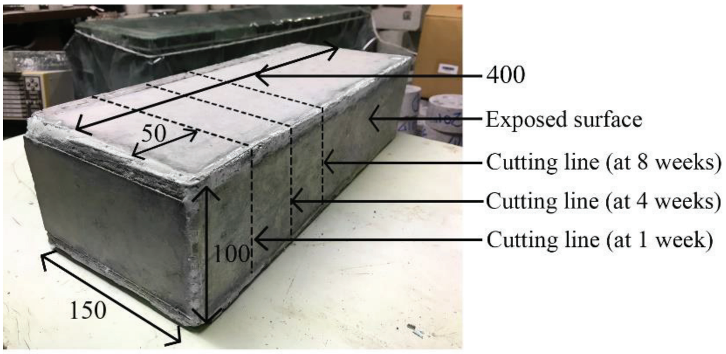

Unit: millimeter

Fig. 12 Concrete specimen configuration for accelerated carbonation test

Table 5 Summary of specimens

Tested	Type	Size (mm)		No. (each mixture proportion)	Age (days)
		Prismatic (w×h×l)	Cylindrical (Ø×h)		
Temperature monitoring	Mortar	40×40×160		2	58
	Concrete	100×100×150		2	58
SEM examination	Mortar	10×10×20			
Porosity examination	Mortar	Free shape, size between 2.36-4.75		1	58
Compressive strength	Mortar		5×10	3	28, 58
	Concrete		100×200	3	28, 58
Splitting tensile strength	Mortar		5×10	3	28, 58
	Concrete		100×200	3	28, 58
Electrical resistance measurement	Mortar	40×40×160		1	58
	Concrete	100×100×150		1	58
Carbonation test	Mortar	80×40×160		1	58
	Concrete	100×150×400		1	58
CH examination	Mortar	Powder, size less than 150×10^{-3}		1	58
	Concrete			1	58
Chloride penetration	Mortar	40×40×160		1	58
	Concrete	100×100×150		1	58

3.2.3. Curing and pretreatment

Mortar and concrete were mixed in a mixer, in laboratory, and were casted in prepared mold. All top surfaces were covered with plastic sheets and wet cloths to prevent water evaporation, and then stored at 20°C and 60% of relative humidity (RH). At 24 h after casting, all of specimens were demolded and cured in water at 20°C for 27 days, and then stored at 20°C and 60% RH for 30 days; this was done to reduce free water in the capillary pores, which would otherwise allow for a buildup of pore pressure during the heating test, and consequently, spalling or explosion (Ozawa and Morimoto 2014; Lu 2015). In the case of a fire, one surface of a concrete structure is generally exposed to fire. Therefore, one day before heating, five surfaces (all but one) of each specimen were covered with five layers of aluminum adhesive tape and insulation materials to simulate the conditions of a real fire. Aluminum adhesive tape was used for the first, third, and fifth layers to prevent the moisture evaporation from the sides of the specimen. Two types of insulation materials, rock wool and silica aerogel, were used for high temperature protection. The silica aerogel insulation material, a high quality insulation material, was used for the second layer. Meanwhile, the rock wool insulation material was used for the fourth layer to ensure that the high temperature could not affect the sides of the specimen.

The unheated specimens were cured in water at 20°C for 27 days and stored at 20°C and 60% RH for 30 days, similar to the heated specimens; subsequently, five surfaces of the unheated specimens were covered with aluminum adhesive tape in one layer to prevent the moisture absorption or migration from the sides as a reference.

3.3 Heating regime

A hot plate was used in this study for rising up the temperature at the surface of specimens to 350°C of which temperature was chosen to prevent dehydration of CH (Lin et al. 1996; Georgali and Tsakiridis 2005; Omer 2007; Rongviriyapanich et al. 2016). Furthermore, the Architectural Institute of Japan standard (2015) even suggests that concrete exposed to this heating level, 350°C, do not require repair.

At the age of 58 days, the uncovered surfaces of the specimens were exposed to high temperature by placing these on a hot plate as seen in **Fig. 13**. The temperature of the hot plate was raised up to 350°C at a rate of approximately 20°C/min and kept at 350°C for 15 min. The maximum temperature and heating rate were chosen because Lin et al. (1996) reported that the temperature at 350°C with a rate of 20°C/min were not enough to dehydration of CH and generate large cracking. After that, the specimens were removed from the hot plate for testing. The total heating time was approximately 31 min. The temperature at a hot plate was monitored by thermocouple during testing.

Fig. 13 Heating specimens on hot plate

3.4 Scanning electron microscope (SEM) examination

The microstructure of mortar specimens was changed due to high temperature such as micro-cracking. To investigate the microstructure of heated and unheated mortar specimens, scanning electron microscope (SEM) was used. The heated mortar specimens for temperature monitoring were collected three days after heating (i.e. at the age of 61 days) and cut at the depths of 2.5, 20 and 40 mm from the exposed surface into 10 mm width, 10mm height and 20 mm length. For the unheated specimens, the specimens at the age of 61 days were cut into the same size at the center of the specimens.

3.5 Porosity examination

At the age of 58 days, after heating, all of the aluminum adhesive tape and insulation materials were removed from the mortar specimens, which were cooled naturally at 20°C and 60% RH. The mortar specimens were cut at the interval of 20 mm from the exposed surface, crushed to 2.36-4.75 mm, and then soaked in acetone and put in a desiccator at -0.1 MPa for 1 h to stop further hydration reaction. Then, the specimens were kept in acetone before being measured by mercury intrusion porosimetry (MIP).

Subsequently, the acetone was drained from the sample by using a desiccator for 24 h. The 58-day-old mortar specimens before heating were prepared similarly. The porosity of the mortar specimens was studied using MIP.

3.6 Compressive strength and splitting tensile strength test

The compressive strength test of three cylindrical specimens was conducted at the ages of 28 and 58 days as per JIS A1108 (Method of test for compressive strength of concrete). The average value of three specimens was recorded as a compressive strength. At the age of 58 days, the test was carried out on the heated specimens before and after heating. The insulation material of specimen for conducting were removed and all of the aluminum adhesive tape also. Then, the specimens were cooled down naturally at 20°C and 60% RH to prevent from the thermal shock before further testing. The aluminum adhesive tape was removed from the unheated specimen also.

The splitting tensile test was conducted on the concrete specimen at the ages of 58 days. The average value of 3 specimens was recorded for the splitting tensile strength.

3.7 Moisture transfer examination

After the aluminum adhesive tape of the third and fifth layers and all insulation materials were removed from the heated mortar and concrete specimens, moisture transfers in heated specimens were immediately measured at 20°C and 60% RH for 120 days. The unheated mortar and concrete specimens were covered with single layer of aluminum adhesive tape and stored in the same place, and the moisture transfers were also measured at the same time.

Because concrete conductivity is correlated with water content, the moisture transfer in mortar and concrete specimens was assessed by measuring electrical resistance as a function of time through stainless steel rods. The electrical resistance at each depth from the exposed surface was measured using an inductance capacitance resistance (LCR) meter. The electrical resistance was recorded at the specific times.

3.8 Electrical resistance measurement

Concrete is a conductive material owing to ionic movement occurring inside it; thus, it can hold electrical charge. Electrical resistivity is measured from the resistance of concrete when electrical current passes through it. Direct current (DC) can induce polarization that affects the stainless steel rod-concrete interface and pore-solution to solid-phase interface. Therefore, the DC current cannot be measured stably. On the other hand, when concrete is subjected to alternating current (AC), the dipoles of ions in pore solution can direct the electric current (Layssi et al. 2015), resulting in stable measurement. Thus, AC is appropriate for measuring electrical resistance.

Madhavi and Annamalai (2016) and Layssi et al. (2015) reported many configurations to measure electrical resistivity of concrete. The two-point uniaxial technique has been widely used for this purpose (Elkey and Sellevold 1995; Layssi et al. 2015; Madhavi and Annamalai 2016) and was also used in the present study. Layssi et al. (2015) reported that an electrical frequency of 0.5 – 10 kHz is appropriate to obtain the real resistance of concrete using the two-point uniaxial technique. Elkey and Sellevold (1995) also reported that the difference in the electrical resistance of concrete for variable electrical voltage (V) disappeared when applying at least 1 kHz of electrical frequency. AC with 1kHz frequency and 1 V was used in this study.

3.9 Electrical resistivity calculation

In the two-point uniaxial technique, electric current between two electrodes, i.e., stainless-steel rod in the present study, passes through concrete and the electrical resistance is measured. The stainless-steel rods (electrode) in this study were inserted into the mortar and concrete specimen to ensure a proper electrical connection during the measurements. Equation (1) describes the relation between the resistivity and resistance:

$$\rho = k \cdot R \qquad (5)$$

where,

ρ: electrical resistivity (kΩ·cm)

k: geometrical factor (cm)

R: electrical resistance (kΩ)

The geometrical factor depends on the size and shape of the specimen as well as the distance between the stainless-steel rods. In the two-point uniaxial technique, the geometrical factor is

$$k = \frac{\pi \times l}{\log\left(\frac{d}{a}\right)} \qquad (6)$$

Where,

l: depth of electrode (cm)

d: interval of electrode (cm)

a: electrode radius (cm)

Finally, the electrical resistivity in expressed as

$$\rho = \frac{\pi \times l}{\log\left(\frac{d}{a}\right)} \times R \qquad (7)$$

3.10 Accelerated carbonation test

Similar to the moisture transfer examination, after removal of the aluminum adhesive tape of the third and fifth layers and all insulation materials and then the cooling period, the heated mortar specimens were stored at 20°C, 60% RH, and 5% concentration of CO_2 for an accelerated carbonation test as per the JIS A 1153 standard test method of accelerated carbonation for concrete. The unheated specimens were also stored under the same conditions as the heated specimens. The specimens were cut at every 20 mm (Fig. 9) for mortar specimen and 50 mm for concrete specimen (see Fig. 12) from the side edge perpendicular to the exposed surface after 1, 4, 8, 13, and 26 weeks. Then, the carbonation depths of the cut surface were measured using phenolphthalein. The average of 10 measurements of carbonation depth was recorded for the mortar specimens and 20 measurements for concrete specimens.

3.11 Calcium hydroxide examination

The accelerated carbonation test method was used in this study to assess the durability of postfire concrete. Generally, CO_2 in atmosphere diffuses into concrete and can react with calcium hydroxide $Ca(OH)_2$ (CH) and calcium silicate hydrate $3CaO.2SiO_2.3H_2O$ ($C_3S_2H_3$), in the presence of moisture.

$$Ca(OH)_2 + CO_2 \rightarrow CaCO_3 + H_2O \qquad (8)$$

$$3CaO.2SiO_2.3H_2O + 3CO_2 \rightarrow 3CaCO_3 + 2SiO_2.H_2O + 2H_2O \qquad (9)$$

The availability of calcium oxide (CaO) also affects carbonation as shown in equation (6). Especially, when concrete is exposed to high temperature, it undergoes greater deterioration of the hydration products, thus potentially producing more CaO for the reaction, as seen in equation (7).

$CaO + CO_2 \rightarrow CaCO_3$ (10)

$Ca(OH)_2 \rightarrow CaO + H_2O$ (11)

Therefore, in this study, we observed that CH did not produce CaO after heating. There is a molecule of water in the chemical structure of CH that vaporized at a high temperature. Therefore, TG/DTA was used to determine the remaining amount of CH in the mortar specimen.

As in the compressive strength test specimens, all of the aluminum adhesive tape and insulation materials were removed after heating and the mortar specimens were left to cool at 20°C and 60% RH. The aluminum adhesive tape of the unheated mortar specimens was also removed. Powder samples of the heated mortar specimens were collected at depths of 2.5, 20, 40, 60, and 80 mm from the exposed surface by drilling with diameter 6 mm. For the unheated specimens, samples were collected at the center of the specimens and then pulverized. The powder samples were passed through a 150 μm sieve, and then soaked in acetone and put in a desiccator at -0.1 MPa for 1 h to stop further hydration. Then, the specimens were kept in acetone. Subsequently, the samples were dried in a desiccator for 24 h before testing.

3.12 Accelerated chloride penetration

As in the compressive strength test, after removal of all of the aluminum adhesive tape and insulation materials, the mortar specimens were left to cool at 20˚C and 60% RH. The aluminum adhesive tape of the unheated specimens was also removed. Five surfaces of both heated and unheated specimens were covered with epoxy resin so that the chloride ions penetrate the specimens in one direction. After coating, the specimens were stored at 20˚C and 60% RH for 1 day to ensure the setting of the resin. The uncovered surface of heated and unheated specimens was then immersed in a 3% sodium chloride solution (NaCl) for 1 day before being dried for 6 days. This cycle was selected because the pretest results. For pretest, the dummy specimens, mortar and concrete, were immersed in NaCl solution for 1 day then they were dried at 20˚C and 60% RH until they became constant mass. It takes 6 days for this process. These wet and dry operation were repeated 45 times.

The chloride penetration depth in the mortar and concrete specimens was measured at the fifteenth, thirtieth and forty fifth cycles by using silver nitrate solution. The average value of 10 measurements of chloride penetration depth was recorded for the mortar specimen and 20 measurements for concrete specimen.

4. Mechanical properties

An experimental study in this chapter has been conducted in order to study properties related to microstructure and strength of mortar and concrete, with and without addition of PP fibers, after heating. The results of temperature inside the specimens are shown to indicate the maximum temperature. Then, the images of SEM and total pore volume of heated and unheated mortar specimen are investigated to observe the changing in microstructure. Finally, the strengths of mortar and concrete are summarized and discussed.

4.1 Temperature history

Fig. 14-Fig**. 16** show the temperature of the hot plate during heating and the internal temperature of the mortar specimens for 60 min after the beginning of heating. The temperature history of the concrete specimen is shown in and Fig. 17-Fig**. 19** The temperature history of the hot plate is slightly different for each mixture because heating is controlled manually and separately for each mixture. When the mortar and concrete specimens are exposed to high temperature, the internal temperature at each depth gradually increase with exposure time.

Compared to the C035 and C045 specimens, the temperature of the C035PP fluctuated slightly from 150 to 180˚C at 2.5 mm depth. This is due to the melting of PP fibers in the specimen because the melting point of PP used in this study is around 160˚C. Table 6 lists the rates of temperature increase at depths of 2.5, 20 and 40 mm for the mortar and concrete specimens, which were determined by linear regression between 0-31 minutes of the heating time. Although the rate of temperature increase at 2.5 mm for C035PP specimen is higher than that for the C035 specimen, the rates at 20 and 40 mm for C035PP specimen are lower than those for the C035 specimen. Heating energy might be consumed by the melting of PP fibers in C035PP.

Table 6 The rate of internal temperature increase in mortar and concrete specimens

Name		The increasing rate at the depth from exposed surface (°C/min)		
		2.5 mm	20 mm	40 mm
Mortar	M035	6.57	4.03	2.64
	M045	6.99	4.25	2.62
	M035PP	7.32	5.22	3.24
Concrete	C035	7.50	6.23	3.85
	C045	6.47	5.13	2.84
	C035PP	8.96	4.34	3.37

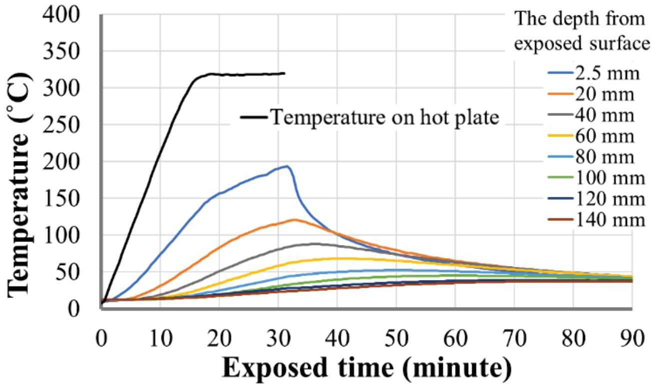

Fig. 14 The temperature history of hot plate during heating and the internal temperature of M035

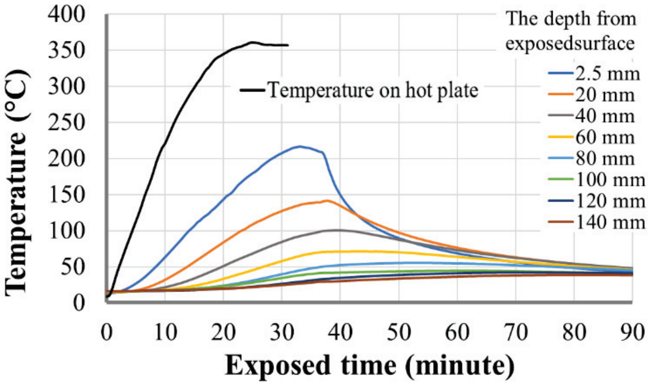

Fig. 15 The temperature history of hot plate during heating and the internal temperature of M045

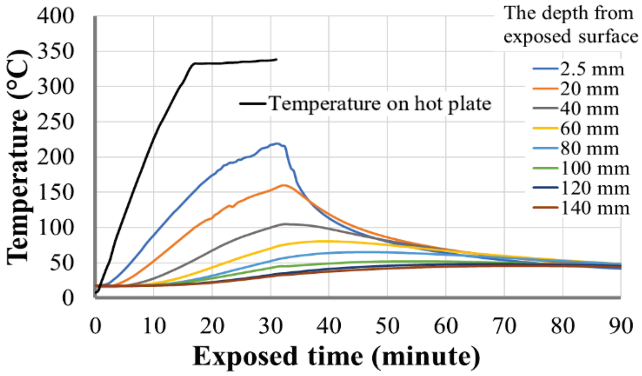

Fig. 16 The temperature history of hot plate during heating and the internal temperature of M035PP

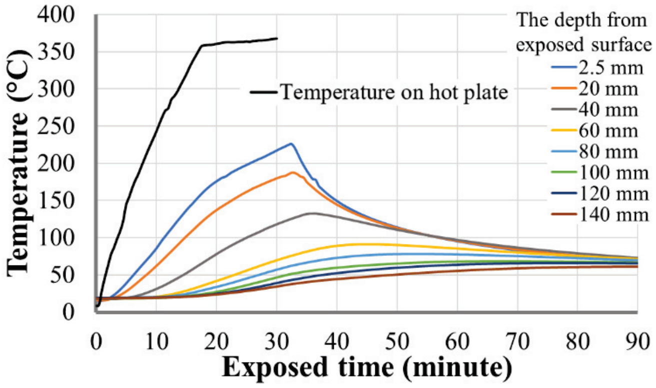

Fig. 17 The temperature history of hot plate during heating and the internal temperature of C035

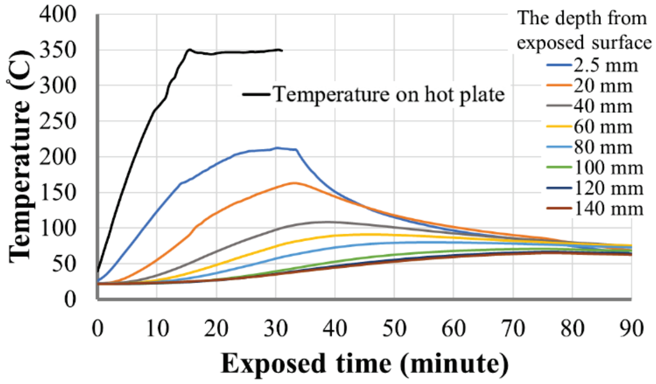

Fig. 18 The temperature history of hot plate during heating and the internal temperature of C045

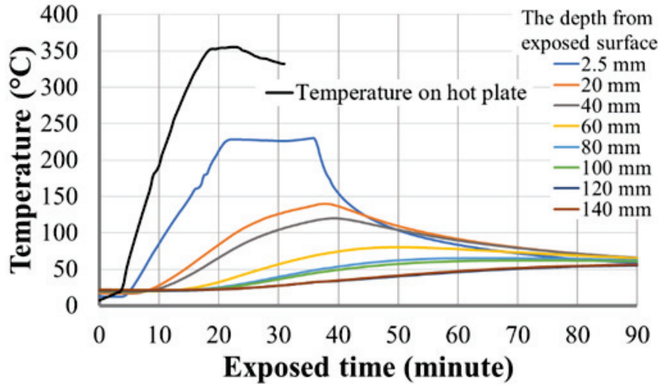

Fig. 19 The temperature history of hot plate during heating and the internal temperature of C035PP

4.2 SEM observation

The microstructure of the mortar specimens is observed with an SEM, and the images are shown in Fig. 20-Fig**. 22**. Fig. 20(b) and (c), Fig. 21(b) and (c), and Fig. 22(e) show microcracks formed in the M035, M045 and M035PP specimens after heating, respectively. Cracking occurred in the mortar at depth of 2.5 and 20 mm where the internal temperatures were approximately 200°C and 150°C, respectively. However, microcracks were not observed at a depth of 40 mm in the mortar specimens.

Fig. 22 (a-e) shows PP fibers and microcracking in the M035PP specimen. The chemical composition of PP fibers from SEM observation is shown in Table 7. The images show that the diameter of the PP fibers at the depths of 2.5 and 20 mm decreases to approximately 35 and 32 μm, respectively, possibly because a part of the PP fiber melts at depths of 2.5 and 20 mm, where the temperatures are approximately 200°C and 150°C, respectively. Additionally, the losing of PP fibers due to melting also can be observed by visual inspection as seen in Fig. 23. However, the temperature of 150°C is not consistent with the melting point of PP fibers, i.e., 160°C. The observed change in Fig. 22(c), Fig. 23 and the temperature profile suggest that the temperature of the thermocouple in the M035PP specimen at a depth at 20 mm depth is affected by the melting of PP fibers, as mentioned in Section 4.1. At the depth of 40 mm, PP fibers do not melt because their diameter is approximately 49 μm, as shown in Fig. 22(d).

The melting of PP fibers create pressure-induced tangential spaces (PITS) (Ozawa and Morimoto 2014), as shown in Fig. 24.

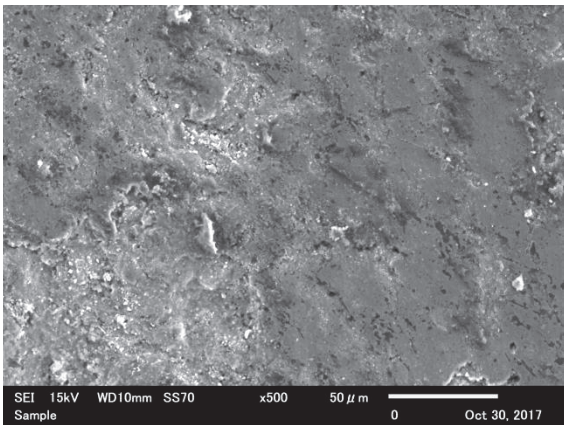

a) M035 before heating

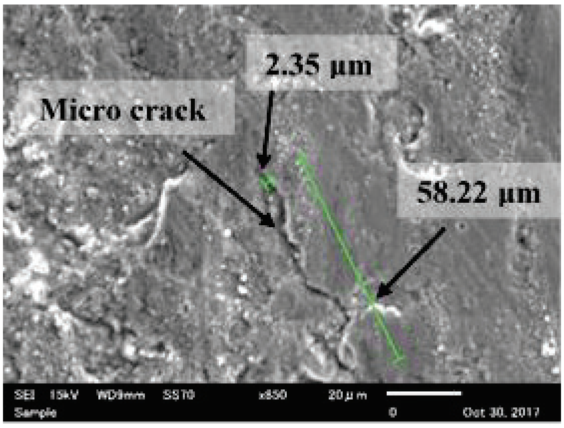

b) M035 at the depth of 2.5 mm from exposed surface after heating

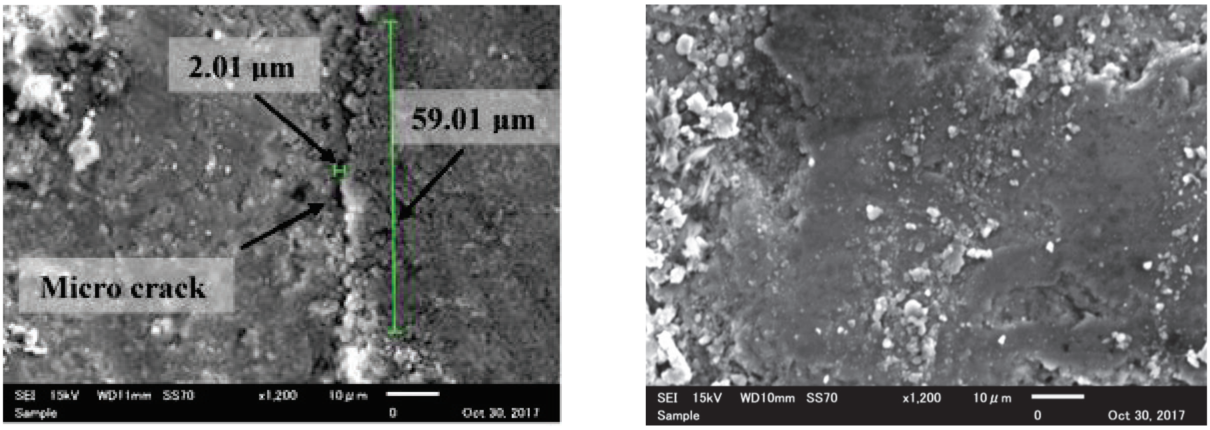

c) M035 at the depth of 20 mm from exposed surface after heating

d) M035 at the depth of 40 mm from exposed surface after heating

Fig. 20 SEM images of mortar specimen with W/C of 0.35 before and after heating

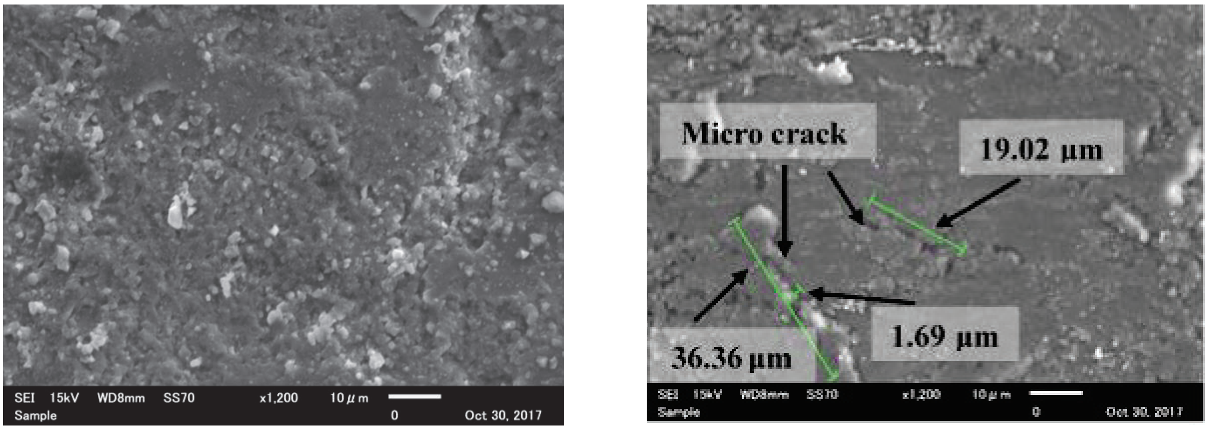

a) M045 before heating

b) M045 at the depth of 2.5 mm from exposed surface after heating

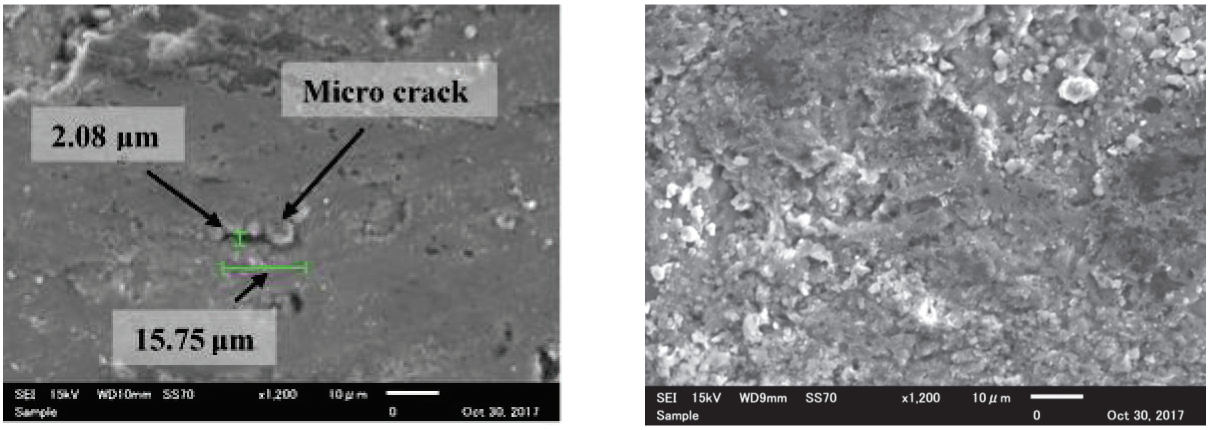

c) M045 at the depth of 20 mm from exposed surface after heating

d) M045 at the depth of 40 mm from exposed surface after heating

Fig. 21 SEM images of mortar specimen with W/C of 0.45 before and after heating

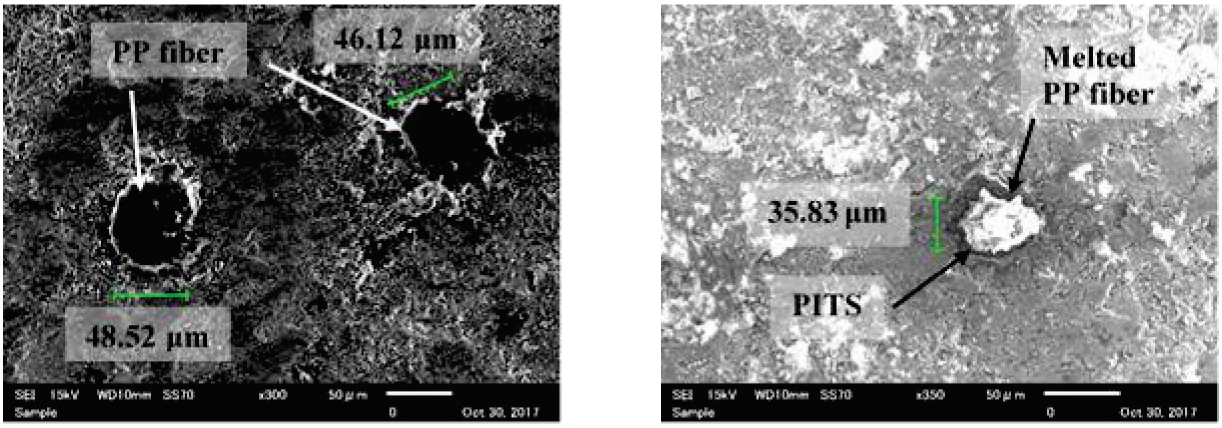

a) M035PP before heating

b) M035PP at the depth of 2.5 mm from exposed surface after heating

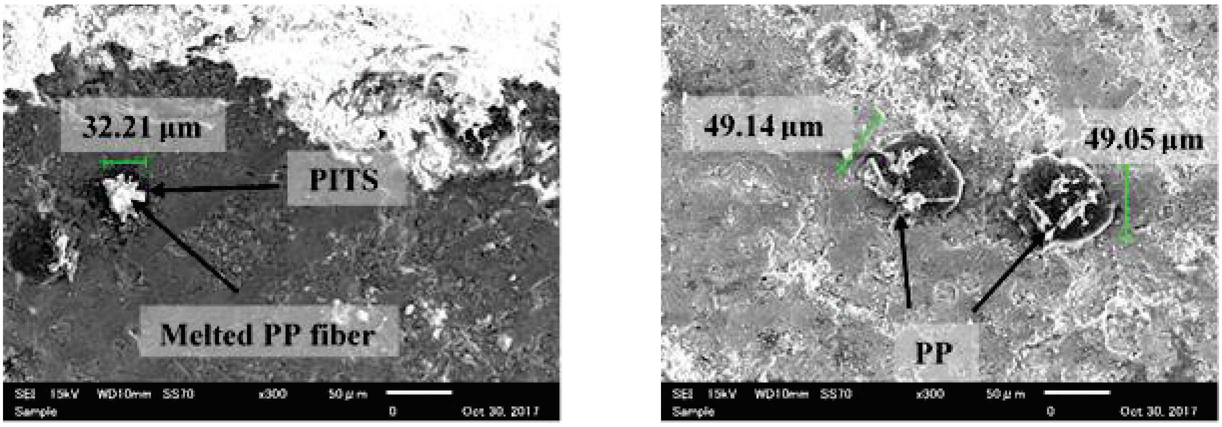

c) M035PP at the depth of 20 mm from exposed surface after heating

d) M035PP at the depth of 40 mm from exposed surface after heating

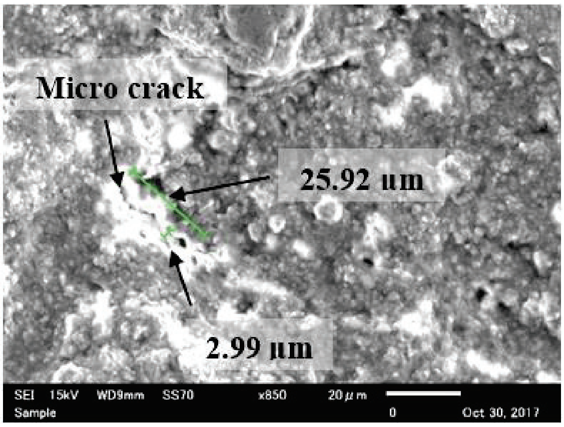

e) Micro-crack at the depth of 2.5 mm from exposed surface of M035PP after heating

Fig. 22 SEM images of mortar specimen with W/C of 0.35 and PP fibers before and after heating

Table 7 Chemical composition of PP fibers

Chemical	Percentage by mass
C	72.58
O	13.87
Al	0.47
Si	0.94
S	0.18
Ca	1.55
Pd	2.02
Pt	8.39
total	100.00

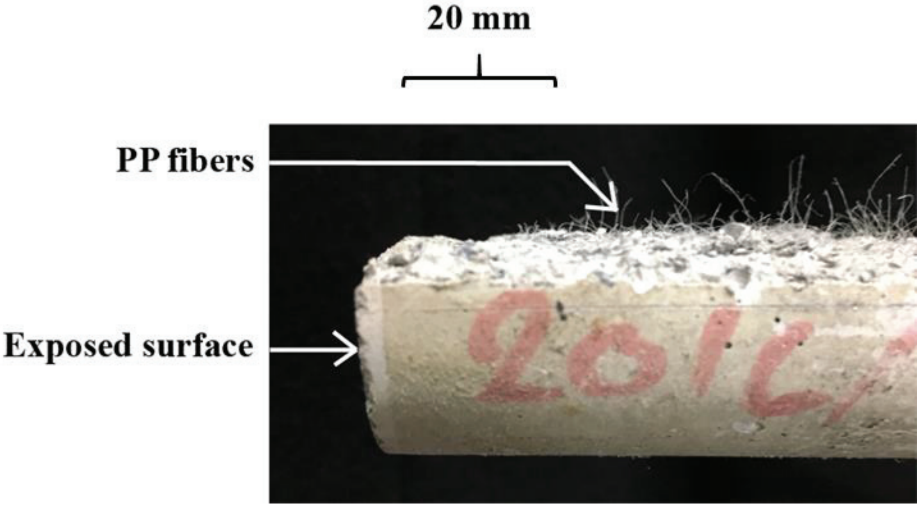

Fig. 23 Melting of PP fiber observed by visual inspection

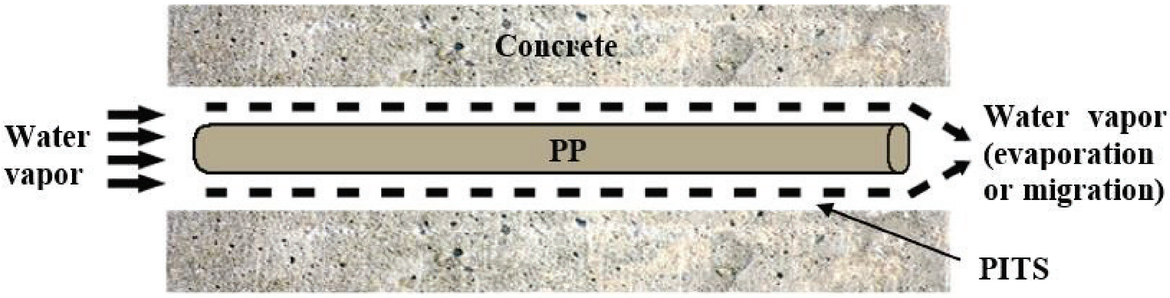

Fig. 24 Pressure–induced tangential spaces (PITS)

4.3 Porosity of specimens

4.3.1. Mortar specimens

Fig. 25(a)-(c) shows the pore volume of the M035, M045 and M035PP specimens at 58 days, before and after heating. The diameter of pores is divided into the following three ranges: 0.006–0.1, 0.1–1 and 1–10 µm. For the unheated specimens, the pore volume of the M045 specimen is higher than those of the M035PP and M035 specimens. After heating, the pore volume at 0–20 mm from the exposed surface for all heated specimens clearly increased. The volume increments in the pores of 1 – 10 µm in diameter for the heated M035, M045 and M035PP specimens are 200%, 174% and 304%, respectively. This suggests that the microcracks generated by pore pressure occur at this depth, and their widths, as estimated from the SEM images of all heated specimens, are approximately 2 – 3 µm. At 20 – 40 mm from the exposed surface of the M035 specimen, the pore volume also increases, especially in the range of 0.1 – 1 µm, and the volume in this range is higher than that at the depth of 0 – 20 mm. However, the volume in this range at the depth of 20-40 mm is smaller than that at the depth of 0-20 mm, in the M045 and M035PP specimens. This suggests that the increase in pore volume in the M035 specimen is also due to pore pressure-induced cracks. The dense microstructure of mortar with a low W/C prevents water vapor from easily transferring during heating, increasing the pore pressure and generation of micro-cracks. Thus, the increase in pore volume is not observed in the M045 specimen. For the heated M035PP specimen, the increase in pore volume is caused by not only microcracks but also PITS. This explains why the volume increase in the M035PP specimen of pores with 1-10 µm in diameter are higher than those in the M035 specimen. However, the pore volume at 20-40 mm depth does not increase, which suggests that the PP fibers do not melt.

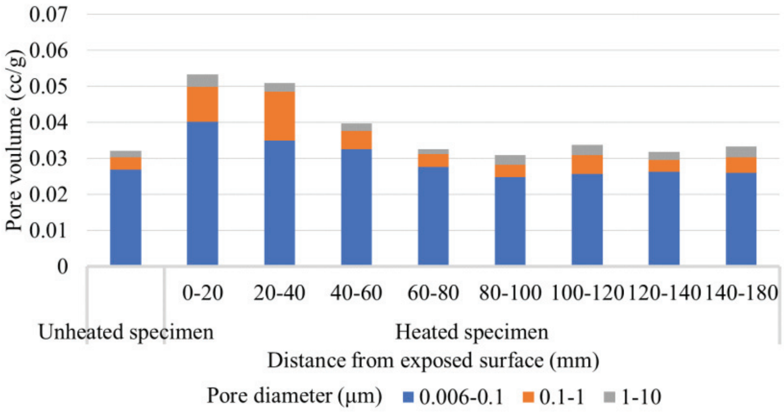

a) The porosity of M035

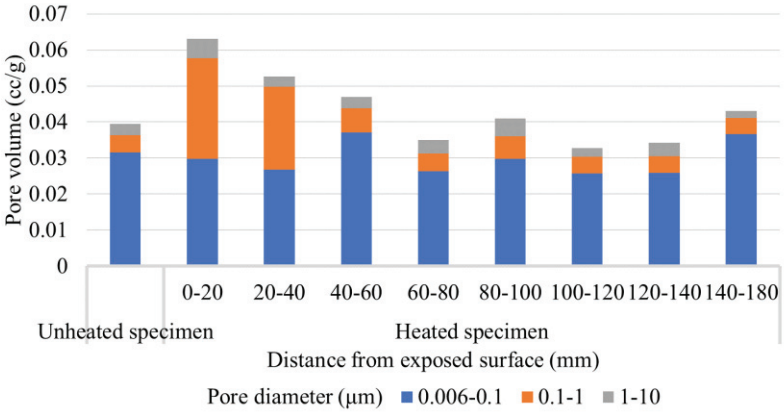

b) The porosity of M045

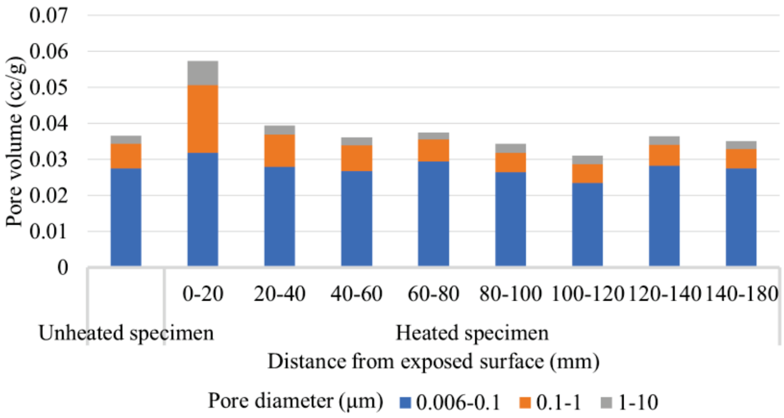

c) The porosity of M035PP

Fig. 25 The porosity of mortar specimens

4.4 Compressive strength

4.4.1. Mortar specimens

Table 8 shows the compressive strengths of mortar specimen, M035, M045 and M035 PP, at the ages of 28 and 58 days. The results at 58 days include the compressive strengths before and after heating. For the unheated specimens, at 58 days, the compressive strength of the M035 and M035PP specimens are approximately 75 MPa and that of the M045 specimen is approximately 60 MPa. There was observed that the PP fibers did not increase compressive strength in the mortar specimen with PP fiber before heating. Behnood and Ghandehari (2009) and Noumowe et al. (2009) also reported that the used of PP fiber and the increase in a dosage of PP fibers do not have a significant effect on the compressive strength of concrete.

After heating to approximately 330°C, the compressive strengths of the M035, M045, and M035PP specimens decreased to approximately 63, 43, and 65 MPa, which correspond to 83, 72, and 85% of the compressive strength of the unheated specimens, respectively. The reduction in compressive strength of the mortar specimen after exposure to 330°C could explained as follows: some of the moisture inside the mortar specimen evaporates, which then migrates deeper into the specimen and builds pore pressure. When the pore pressure exceeds the tensile strength of mortar, crack stars to occur, and the strength drops sharply, as seen in SEM images in Section 4.2.

4.4.2. Concrete specimens

For the concrete specimens, the compressive strengths of C035, C045, and C0358PP specimens are listed in Table 8. For the unheated specimens, at 58 days, the compressive strengths of C035, C045, and C035PP specimens are approximately 75, 63, and 82 MPa, respectively. Although the compressive strength of C035PP specimen is higher than that of C035, the difference in compressive strength between them was less than 10%. Apparently, the PP fiber do not affect the compressive strength of concrete with the same W/C.

After heating, the compressive strengths decreased and the residual compressive strengths of the C035, C045, and C035PP specimens are approximately 56, 52, and 70 MPa, respectively, which corresponds to 75, 82, and 85% of the compressive strength of the unheated specimens.

The reduction in compressive strength of the concrete specimen is due to pore pressure-induced cracks, as mentioned in Section 4.2.

Regarding the unheated specimens, the compressive strength at each age of the concrete specimens is higher than that of the mortar specimens with the same W/Cs except for M035 and C035 specimens. Meanwhile, for the heated specimens, the percentage of residual compressive strengths of C035 specimen is lower than that of M035 specimen. The differential thermal expansion between cement paste and coarse aggregate at the internal temperature between 100-220°C is a reason for the reduction, which can affect the residual compressive strengths of concrete (Behnood and Ghandehari 2009; Yermak et al. 2017; FIB 2007).
However, the thermal incompatibility problem was mitigated by the free space generated by the melting of PP fibers. This is the reason why the residual compressive strength of the concrete specimen with PP fibers is higher than that of the concrete specimen without PP fiber and the residual compressive strength is almost the same in the mortar specimens.

Table 8 The compressive strength of the mortar and concrete specimens

	Name	Compressive strength (MPa) (S.D.)		
		28 days	58 days	
			Before heating	After heating
Mortar	M035	75.22 (3.71)	75.87 (0.96)	63.16 (0.64)
	M045	38.97 (0.46)	60.27 (1.35)	43.31 (1.89)
	M035PP	63.38 (2.19)	77.70 (1.32)	65.87 (1.33)
Concrete	C035	66.98 (0.29)	75.01 (1.32)	56.10 (0.85)
	C045	59.86 (0.80)	63.66 (2.23)	52.45 (1.92)
	C035PP	69.20 (3.36)	82.48 (0.58)	70.52 (2.17)

S.D.: standard deviation

4.5 Splitting tensile strength test

4.5.1. Mortar specimen

Table 9 shows the splitting tensile strength of mortar specimen, M035, M045 and M035PP, at the ages of 58 days before and after heating. For unheated specimen, splitting tensile strengths of M035, M045 and M035PP specimens were approximately 6.30, 5.50 and 6.40 MPa, respectively. There was observed that the M045 specimens showed the lowest splitting tensile strength due to less density of mortar. Addition of PP fibers was not a significant effect on splitting tensile strength.

After heating, the residual splitting tensile strengths of M035, M045 and M035PP specimens were approximately 5.40, 4.90 and 5.50 MPa, respectively, which corresponds to 86, 89 and 86% of the unheated specimens. The decrease in splitting tensile strength could be explained that was occurred by micro-cracking as discussed earlier in compressive strength section. Generally, tensile strength is more sensitive to macro- and micro-cracks of concrete than is compressive strength. But, this study, the residuals of splitting tensile strength are higher than compressive strength, as seen in Fig. 26. It can be implied that the generated cracks inside the specimen is not much enough to influence the tensile strength of the specimen.

4.5.2. Concrete specimen

For the concrete specimens, the splitting tensile strengths of C035, C045, and C0358PP specimens are shown in Table 9. For the unheated specimens, the splitting tensile strengths of C035, C045, and C035PP specimens were approximately 4.10, 4.30, and 4.20 MPa, respectively, at the age of 58 days. It can be observed that the splitting tensile strength of C035PP specimen was almost same as the C035 specimen. It can be said that PP fibers do not have a significant effect on the splitting tensile strength. And the difference of splitting tensile strength between C035PP and C045 specimens was less than 5%. Generally, concrete is weak in tension, and for NSC, tensile strength is only approximately 10% of its compressive strength and for HSC tensile strength ratio is further reduced.

After heating, the splitting tensile strengths decreased and the residual splitting tensile strengths of the C035, C045, and C035PP specimens were approximately 3.30, 3.30, and 3.70 MPa, which corresponds to 79, 76, and 87% of the unheated specimens, respectively. The reduction of compressive strength of the concrete specimen is due to cracks caused by the pore pressure as mentioned in Section 4.3. It is clearly that the addition of PP fiber can reduce a loss of splitting tensile strength of the heated concrete specimens.

Table 9 The splitting tensile strength of the mortar and concrete specimens

	Name	Splitting tensile strength (MPa) (S.D.)	
		58 days	
		Before heating	After heating
Mortar	M035	6.30 (0.20)	5.34 (0.53)
	M045	5.47 (1.20)	4.87 (0.10)
	M035PP	6.37 (0.65)	5.47 (0.17)
Concrete	C035	4.14 (0.33)	3.26 (0.28)
	C045	4.38 (0.12)	3.34 (0.16)
	C035PP	4.22 (0.07)	3.66 (0.12)

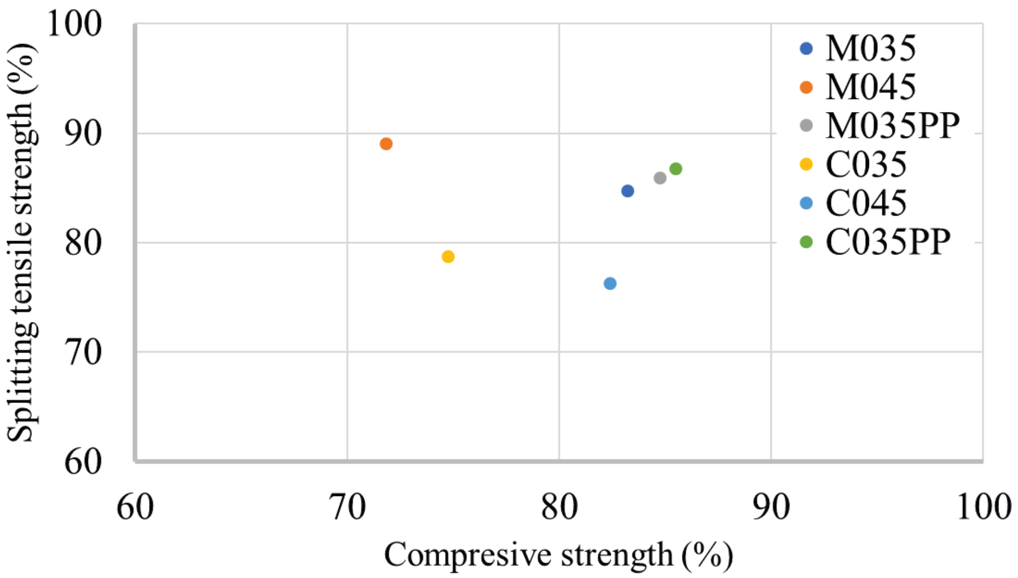

Fig. 26 The residual splitting tensile strength and compressive strength as percentage of those of unheated specimen

4.6 Modulus of elasticity of concrete

The modulus of elasticity is determined as the slope of the best fitting line on the stress-strain curve, as shown in equation 12.

$$E_c = \frac{S_1 - S_2}{\varepsilon_1 - \varepsilon_2} \times 10^{-3} \qquad (12)$$

Where

E_c = Modulus of elasticity of concrete (GPa)

S_1 = Stress at 1/3 of the maximum load (MPa)

S_2 = Stress at 50μ of strain (MPa)

ε_1 = Strain at 1/3 of the maximum load

ε_2 = 50μ

Table 10 shows evaluation of modulus of elasticity of concrete that was calculated from cylindrical concrete specimens. The C035PP specimen showed the highest value at the ages of 28 days and 58 days before heating. There was observed that the modulus of elasticity of all of concrete specimens were increased at the ages of 58 days. Meanwhile, the modulus of elasticity of heated specimens was decreased after heating. As mention in Section 4.4.2, the compressive strength decrease, the modulus of elasticity losses of the C035 and C045 were approximately 4 and 10% compared to those unheated specimens, respectively, while the decrease of specimen with PP fibers (C035PP) was approximately 6% .

The modulus of elasticity of concrete is dependent on moisture content and the microstructure of hydrated cement products in paste. This is the why the modulus of elasticity of heated specimens is lower than the unheated specimen. The result of moisture inside the specimen are shown in next section. Ghosh and Nasser also found that the decrease in elastic modulus was due to a gradual deterioration of the binding matrix with the rise in temperature and it could be associated with micro-cracking observed in micro structure of mortar that is consistent with previous studies (Chang et al., 2006). In the other words, these results are attributed to the loss of moisture due to the heating of concrete and the degradation of microstructure and chemical bonds within concrete, resulting in the development of microcracks. Compared with C035 specimen, the addition of fibers had not significantly degraded of modulus of elasticity.

Table 10 The modulus of elasticity of concrete

Name	Modulus of elasticity (MPa)(S.D.)		
	28 days	58 days	
		Before heating	After heating
C035	37,250.18 (1,267.64)	39,183.91 (1,092.24)	37,511.87 (2,898.92)
C045	33,312.33 (777.12)	38,631.37 (763.11)	34,973.94 (543.06)
C035PP	38,895.20 (369.14)	40,067.50 (932.36)	37,474.10 (288.00)

5. Moisture transfer

This experimental study consists of the results and discussion of moisture transfer inside the specimen. The electrical resistivity method and non-standardized test methods were used to monitor the moisture. All tests were conducted on the specimens in laboratory environment, 20°C and 60%RH. In this chapter a discussion of moisture transfer using electrical resistivity method is given.

5.1 Electrical resistivity of mortar specimen

Fujioka et al. (2013) and Bui et al. (2015) reported that electrical resistance measurements using stainless steel rods can be used to determine the moisture content of the cement paste or mortar owing to the correlation between electrical resistivity and internal RH. Therefore, electrical resistivity is used in this study to examine the moisture transfer in mortar and concrete specimens.

Fig. 27 shows the electrical resistivity of heated and unheated mortar specimens with time. It is observed that the electrical resistivity at 7.5 and 22.5 mm depths for all specimens with and without PP fibers suddenly increased after removal from the hot plate, while that at other depths suddenly decreased, except at 127.5 and 142.5 mm, for the M045 specimen.

The electrical resistivity at each depth for all specimens increased with time. The electrical resistivity of the M035 and M035PP specimens at depths between approximately 60 and 160 mm increased to nearly that of the unheated specimens at each age, except at 82.5 mm depth, for the M035 specimen. However, the electrical resistivity at 37.5 and 142.5 mm depths for the M045 specimen sharply increased to higher values than that of the unheated specimen. The electrical resistivity of the unheated specimens also increases constantly at 58, 118, and 178 days.

5.2 Electrical resistivity of the concrete specimen

The electrical resistivity of the concrete specimens is shown in Fig. 28, where the electrical resistivity of concrete specimens at a depth of 7.5 mm exhibited a behavior similar to that of the mortar specimens. After being removed from the hot plate, the specimens' electrical resistivity at 7.5 mm depth suddenly increased, while that at the other depths suddenly decreased.

The electrical resistivity inside the heated specimens increased, and is higher than that of the unheated specimens at the same age. The electrical resistivity of the unheated specimens also constantly increased at 58, 118, and 178 days.

5.3 Discussion

The changes in the electrical resistivity of the concrete specimens show a similar trend to that of the mortar specimens. Generally, water at the hot surface evaporates first when the temperature reaches 100°C (Jansson 2013; Ozawa and Morimoto 2014; Anderberg 1997; Zdenek 1997). As the temperature increases further, the evaporation process continues. The extremely high electrical resistivity near the exposed surface, where the internal temperatures are approximately 150 to 220°C, suggests that moisture turns into vapor and escaped into the surroundings because the concrete conductivity correlates with the moisture content.

We observe that the microcracks in SEM images and the increase in pore volume in the heated specimen are caused by thermal instability, melting of PP fibers, and high pore pressure. The increase in pore volume of the heated specimens favors the transfer of vapor. In other words, the resistivity at greater depths, where the internal temperatrue is lower than 150°C, is lower than that of the unheated specimen owing to the condensation of the vapor migrating from shallower depth. This suggests that the extremely high electrical resistivity at shallow depths is also caused by the transfer of moisture.

The relations among microcracks, porosity and electrical resistivity are explained as follows: the high porosity at 0 – 20 mm from the exposed surface of all heated specimens facilitates the transfer of vapor, which increase the resistivity at depths of 7.5 and 22.5 mm. On the other hand, at 20 – 40 mm depth in the heated M035PP specimen, the porosity changed slightly, as seen in Fig. 25 (c). Therefore, at this depth, the resistivity of the heated M035PP specimen is lower than that of the M035 and M045 specimens. Compared to the heated M045 specimen at the 0 – 40 mm from the exposed surface, the lower volume of pores 0.1 – 1 µm in diameter of the heated M035 specimen hinders the vapor transfer, resulting in lower electrical resistivity.

For the unheated specimens, the continuous increase in the electrical resistivity of the mortar and concrete specimens at 120 days suggests that the unheated specimen gradually dry when stored at 20°C and 60% RH. This trend is also observed in the heated specimens, at approximately 40–160 mm.

The unheated mortar and concrete specimens in this study were stored at 20˚C and 60% RH after curing. Therefore, the unheated specimens are in a desorption phase when the electrical resistance of the specimens is measured. On the other hands, for the heated specimens, the migration and condensation of water vapor inside the heated specimens can result in an absorption phase in the inside of the specimens. Thus, it could be explained by the hysteresis effect that some electrical resistivities inside the heated specimens are higher than those of the unheated specimens at the same age.

An increase of 1°C at 21°C can reduce 3% of electrical resistivity in saturated surface-dry concrete. In the other hand, under 30% saturation, the electrical resistivity of concrete can be reduced 5%. However, the moisture inside the mortar and concrete specimen changes during heating and the specimens do not remain saturated and surface-dry. The temperature of the heated specimens is increased to 350°C, but their resistivity is higher than that of the unheated specimen, and the electrical resistivity of the heated specimen at a temperature lower than 110°C suddenly decreased after heating. For example, the internal temperature of all mortar specimens at the depth of 60-140 mm 60 minutes after heating (i.e. 90 minutes in the temperature) is approximately 50°C. Therefore, the electrical resistivity should be approximately 40% of the unheated specimen. But the actual electrical resistivity is almost the same as the electrical resistivity of the unheated specimens.

In this study, the electrical resistivity does not decrease with increasing temperature. As a result, the moisture transfer in the concrete and mortar specimens is consistent with the electrical resistivity data. The electrical resistivity increases when the moisture decreases at high temperature. Therefore, in this study, electrical resistivity can be used to investigate the moisture transfer inside the heated specimen without the reduction in electrical resistivity induced by temperature increase.

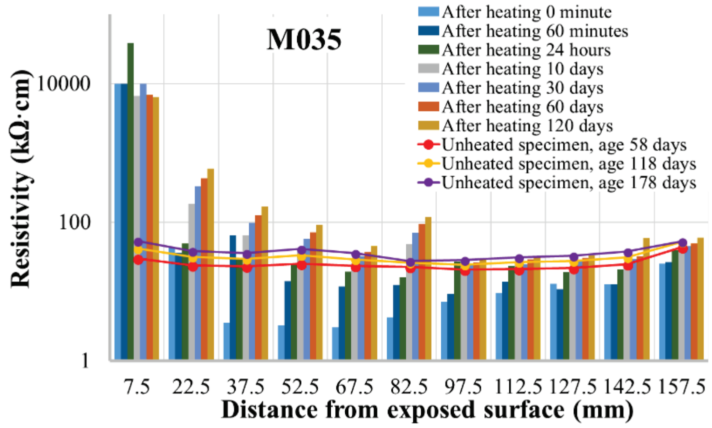

a) The electrical resistivity of M035

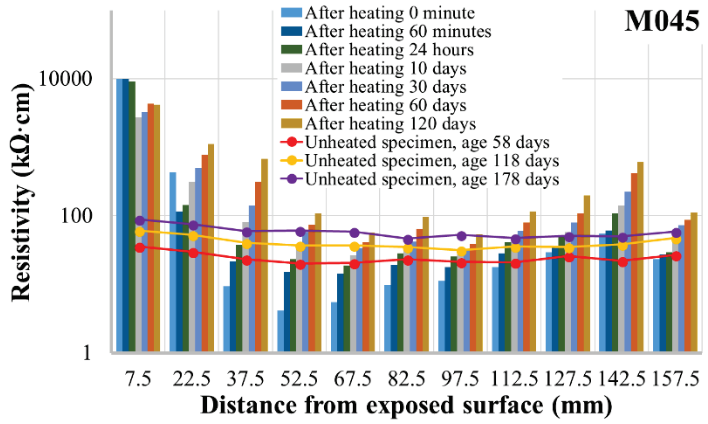

b) The electrical resistivity of M045

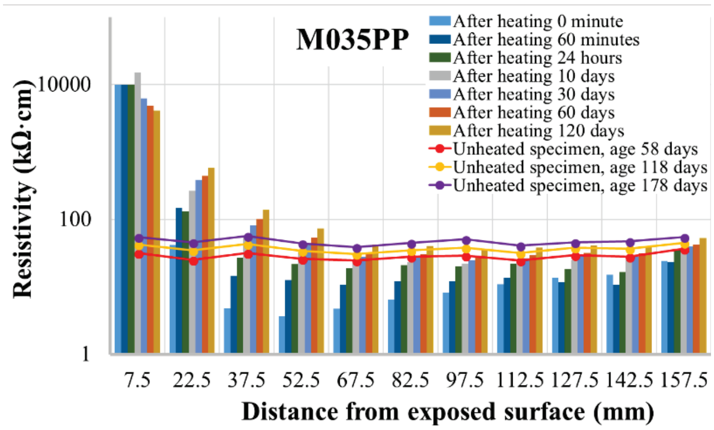

c) The electrical resistivity of M035PP

Fig. 27 The electrical resistivity of mortar specimens

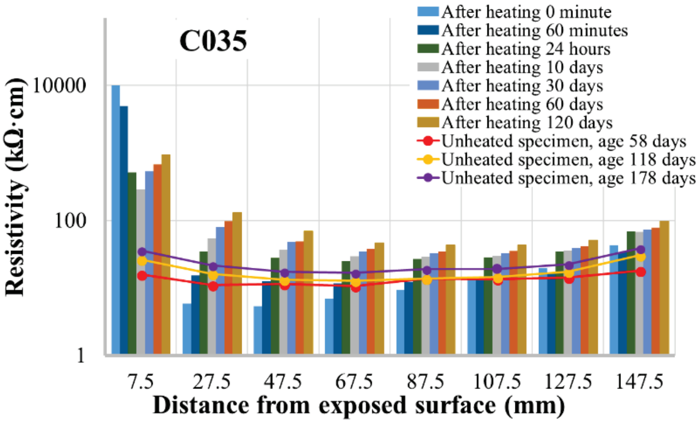

a) The electrical resistivity of C035

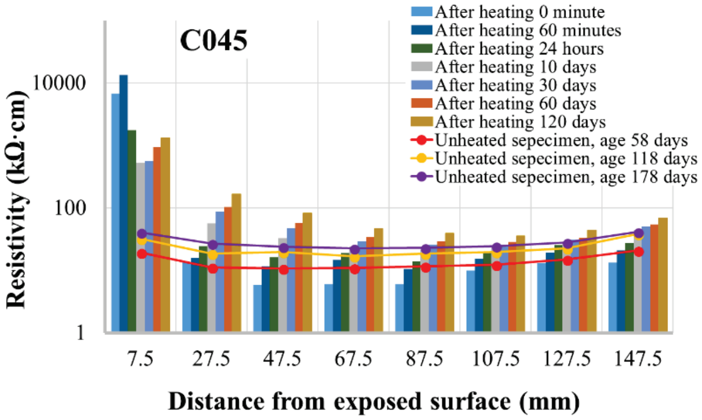

b) The electrical resistivity of C045

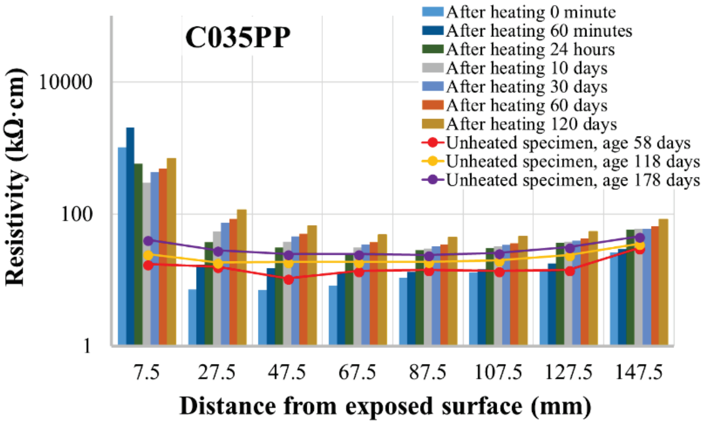

c) The electrical resistivity of C035PP

Fig. 28 The electrical resistivity of concrete specimens

6. The effect of the moisture transfer on durability

The aim of this chapter was to study the influence of moisture transfer and microstructure on residual durability properties of the heated mortar and concrete specimens. Their properties are evaluated by means of standardized test methods. The results obtained in this part are summarized and discussed in this chapter.

6.1 Accelerate carbonation

6.1.1. Mortar specimens

Fig. 29 shows the carbonation depths and rates of both heated and unheated M035, M045, and M035PP specimens. For the unheated specimens, carbonation is not observed for the M035 and M035PP specimens until 13 weeks (i.e., 3.6 √weeks) but it is observed for the M045 specimen after four weeks (i.e., 2 √weeks). The increase in carbonation depth for the unheated specimens is rather small compared to the heated specimens. The carbonation depth for the unheated M035PP specimen is slightly smaller than that for the unheated M035 specimen. Zhang and Li (2013) reported that the addition of PP fibers improves the carbonation resistance of concrete.

For the heated specimens, the carbonation depth of the M035 and M045 specimens is observed one week after heating, while that for the M035PP specimen is observed immediately after heating. It indicates that CO_2 penetrated the heated mortar specimen more easily than the unheated specimen. The electrical resistivity data suggest the formation of a region with very low moisture near the exposed surface of the heated specimen. The pore moisture at this depth is eliminated owing to high temperature. Therefore, the penetration of CO_2 into the heated mortar specimen through the low-moisture content region (i.e., the depth of 0–40 mm) is easier than that in the unheated specimen. The increase in pore volume owing to microcrack and space generation because of melting of PP fibers accelerate the carbonation of the heated specimens. In addition, the carbonation depths in the heated specimens with and without PP fibers increase with time.

The carbonation depths and rate of the heated M045 specimen are slightly higher than those for the M035 specimen because the total pore volume of the M045 specimen is higher than that of the M035 specimen. After heating, microcracks in the M035 specimens occur due to pore pressure, which increase space in the M035 specimen and affects the carbonation depth. The volume of pore of 0.1-1 μm in diameter for the M045 specimen is higher than that for the M035 specimen, which increases the carbonation rate. However, the carbonation depth and rate for the heated M035PP specimen are higher than those for the M035 and M045 specimens. The higher carbonation depth for the specimen containing PP fiber in this study is attributed to the melting of PP fibers, as suggested by the increase in pore volume (i.e., 1-10 μm in diameter). As seen in Fig. 22 (b) and (c), the melted PP fibers created PITS where water vapor can escape and migrate. The free PITS facilitate the penetration of CO_2 and acceleration of carbonation. Noumowe et al. (2009), Bosnjak et al.(2013), Ozawa and Morimoto (2014) and Serrano et al. (2016) reported that the permeability of concrete with PP fibers at 80–170°C increases suddenly and is higher than that of concrete without PP fibers. This study suggests that the higher pore volume of a large pore diameter also affects the carbonation depth and carbonation rate. However, the low values at 8 weeks (i.e. 2.8√weeks) were because carbonation depth was measured at different locations of the same specimen.

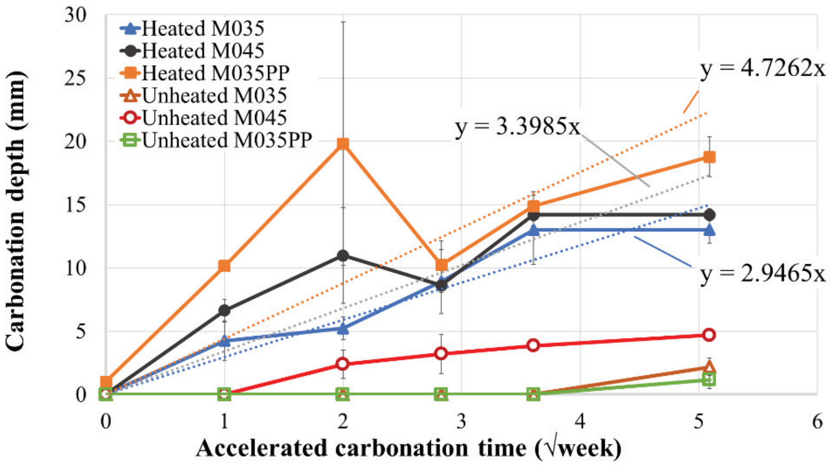

Fig. 29 Carbonation depth and carbonation rate of heated and unheated mortar specimens

6.1.2. Concrete specimen

Fig. 30 shows the carbonation depths and carbonation rates of the heated and unheated specimens for C035, C045 and C035PP. Unheated C035 and C035PP specimens were not carbonated during this period, while carbonation of unheated C045 specimens was observed 1 week after exposed to CO_2. Concrete with a low W/C is more difficult to be carbonated than that with a high W/C because of dense microstructure of concrete and the addition of PP fibers can also improve the carbonation resistance of concrete as mention in previous section.

On the other hands, all heated specimens for C035, C045 and C035PP were carbonated one week after the start of accelerated carbonation test and the carbonation depth increased with the CO_2 exposure time. It indicates that CO_2 penetrated into the heated specimen more easily than into the unheated specimen, regardless of the W/C. The results of SEM and porosity of mortar specimens showed the increase porosity and the generation of pores due to the melting of PP fibers in mortar phase, while the results of the moisture transfer measurement showed the formation of very low moisture condition at the depth closer to the exposed surface due to heating. Considering these results, it is indicated that increased porosity and low moisture content accelerated carbonation of the heated specimens. The carbonation depth of C035PP specimens was almost the same as that of C035 specimen although the porosity of specimen with PP fibers is higher. It could be supposed that melted PP may cover the hardened cement, resulting in contribution to the protection against carbonation.

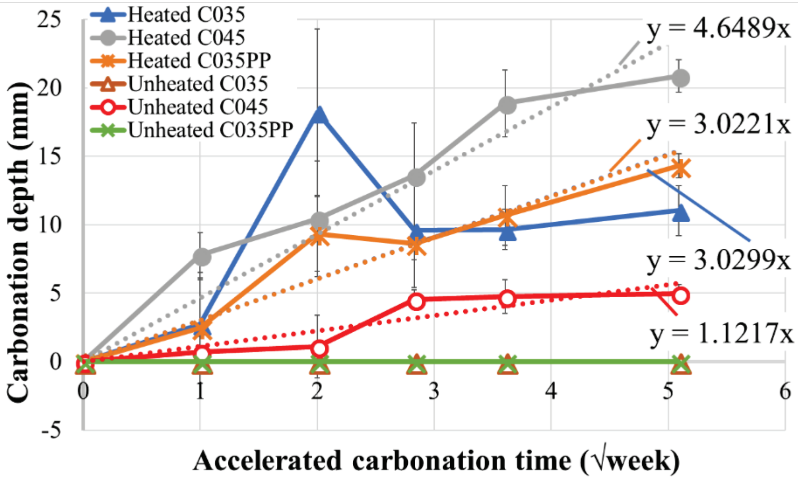

Fig. 30 Carbonation depth and carbonation rate of heated and unheated concrete specimens

6.2 Accelerate chloride penetration

6.2.1. Mortar specimen

Fig. 31 shows the chloride penetration depths of both heated and unheated mortar specimens. Generally, the permeability of high strength concrete is low because of dense microstructure of concrete, especially concrete containing fiber (fib 2007). As a result, the chloride penetration depths of the unheated specimens for M035 and M035PP were observed at 30 cycles, which are approximately 4 and 2 mm, respectively. Meanwhile, the chloride penetration depth of the unheated M045 specimen was observed at 15 cycles, which is approximately 7 mm. Meanwhile, the chloride penetration depths of heated specimen were firstly observed at 15 cycles.

The penetration depths of the heated specimens for M035, M045, and M035PP at 45 cycles were approximately 13, 18, and 20 mm, respectively. Similar to the result of the carbonation, the chloride penetration depth of the heated specimens was larger than those of the unheated specimens due to the low moisture content, high porosity and melting of the PP fibers in the heated region. The region having low moisture content near the exposed surface can absorb NaCl solution more than the unheated specimen because of capillary suction, while high porosity and melting of PP fibers result in easier penetration of chloride ions.

The difference in the chloride penetration rate between the unheated M035 and M045 specimens was caused by the different pore volume, while the influence regions of heating were different in both heated specimens and affected the chloride penetration rate. In addition, chloride penetration depth of both heated and unheated specimens increased with time.

The chloride penetration depth of the heated specimen containing PP fiber was higher than the others because of the generation of spaces due to the melting of PP fibers.

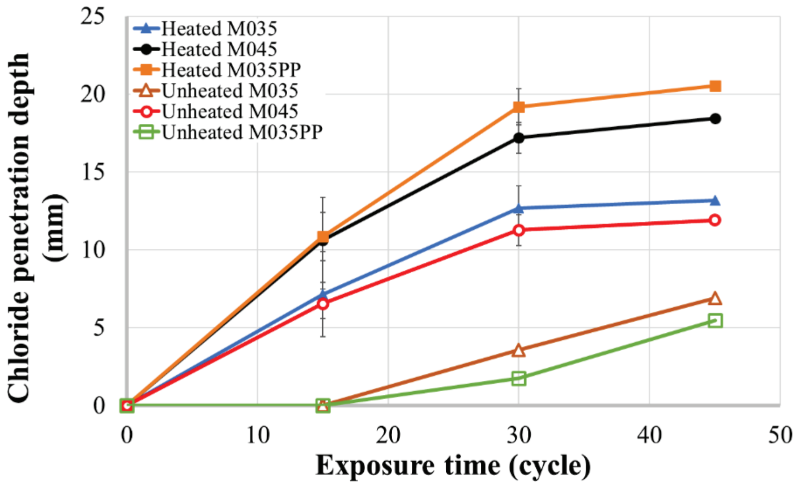

Fig. 31 Chloride penetration depth of mortar specimens

6.2.2. Concrete specimen

The chloride penetration depth of the specimens is shown in Fig. 32. The chloride penetration depth of the unheated specimens for C045 specimen at the age of 30 was approximately 12 mm., while the chloride penetration depth of unheated C035 and C035PP was observed at the age of 45 cycles because of dense microstructure of concrete.

The chloride penetration depths of heated specimens for C035, C045 and C035PP were approximately 23, 34 and 26 mm at 45 cycles, respectively. Similar to the results of the carbonation test, the chloride penetration depths of the heated specimens were larger than those of the unheated specimens. However, the chloride penetration depth of the heated specimen for C035PP was larger than that for C035. The generation of pores due to the melting of PP fibers affected the chloride penetration. Besides, the rates of chloride penetration for the heated specimens were different between 0-15 cycles, 15- 45 cycles, while the chloride penetration depth of the unheated specimen for C045 was almost proportional to the cycle number. This must be related to the influence region of heating, which means the depth of micro-cracks. Also from the difference in the changes of the chloride penetration rates between C035 and C045, the influence region of heating may be different in both mixtures. From the internal temperature profile of C035PP specimen shown in Fig. 19, PP fibers up to the depth of 10 or more millimeters must have been melted. Therefore, chloride penetrated earlier in C035PP specimen than in C035 specimen up to the depth around 20 mm.

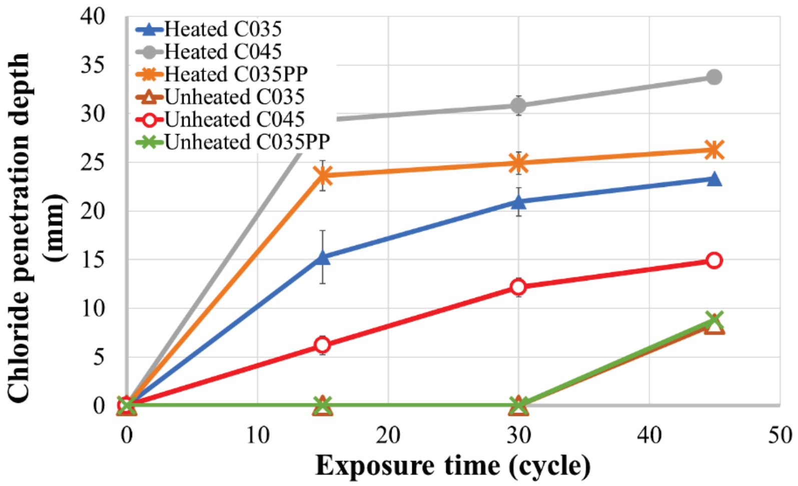

Fig. 32 Chloride penetration depth of concrete specimens

6.3 Amount of calcium hydroxide (CH)

Fig. 33 shows the residual amount of CH of the mortar specimen. The amount of CH of the unheated M035, M045 and M035PP specimens were approximately 7.34, 6.25 and 7.16%, respectively. The CH contents of the M035 with and without PP fibers specimens are almost the same, meanwhile there are higher than the M045 specimen due to the amount of cement. After heating, the residual amounts of CH of the heated mortar specimen were investigated at the ages of 0 min, 12 hr, 1, 2 and 3 days after heating time. The percentages of CH of all heated mortar specimens are quite same as the unheated specimens, approximately different ±10%. It could imply that the CH was not dehydrated by high temperature in this study.

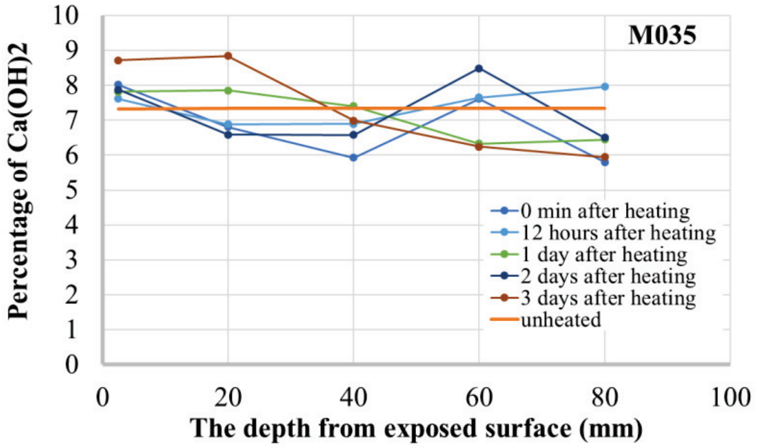

a) Residual amount of CH of M035 specimen

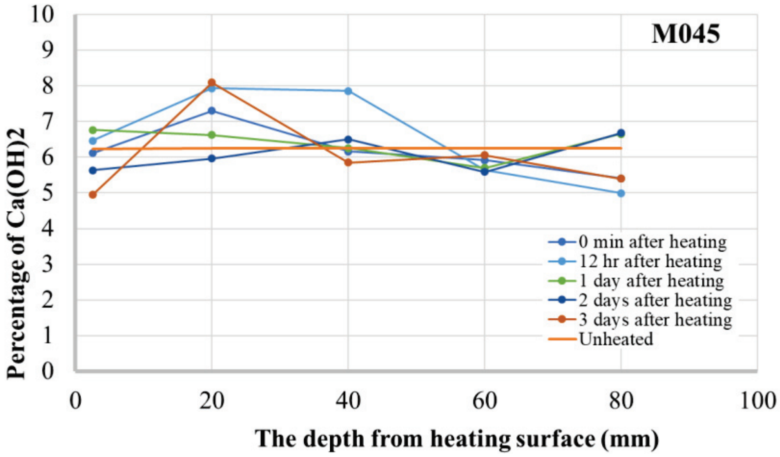

b) Residual amount of CH of M045 specimen

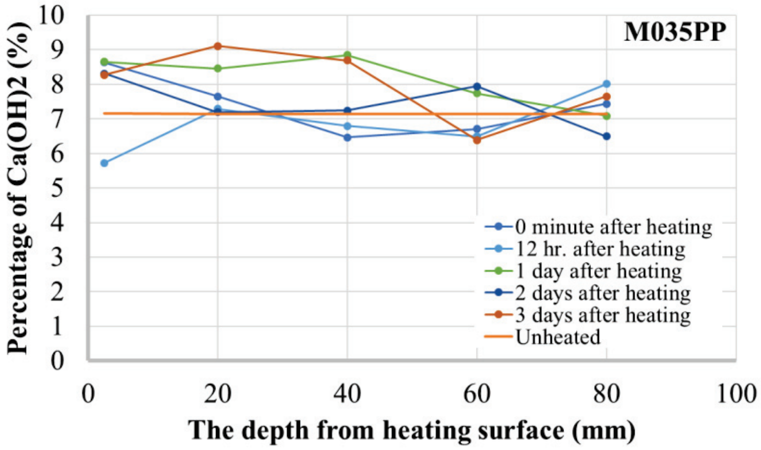

c) Residual amount of CH of M035PP specimen

Fig. 33 Residual amount of CH

7. Conclusions

The conclusions from the experimental results obtained in this study are as follows:

1) High temperature exposure at approximately 350°C reduced the compressive strengths of mortars with W/Cs of 0.35, 0.45, and 0.35 with PP fibers by 17, 28, and 15%, respectively. It also reduced the compressive strength of concrete specimen with W/Cs of 0.35, 0.45, and 0.35 with PP fibers by 25, 18, and 15%, respectively.

2) PP fibers left the pressure-induced tangential spaces (PITS) during heating and could increase the porosity of the mortar and concrete specimens.

3) The electrical resistivity method can be used for the investigation on moisture content and moisture transfer in mortar and concrete after exposed to high temperature at 350°C without multiplying factor for reducing due to the increment of temperature. It also shows that there is a strong correlation between electrical resistivity profile and internal temperature of mortar and concrete specimen. The electrical resistivity increases when the internal temperature is higher than approximate 150°C.

4) The moisture content at depths approximately between 0–40 mm from the exposed surface of the heated mortar specimens with and without PP fibers is lower than that of the unheated specimens. For concrete specimens, the moisture content at depths approximately between 0–50 mm from the exposed surface of the heated specimen is lower than that at the other depths. The region of mortar and concrete specimens at the depths far from the exposed surface gradually dries with time.

5) The low moisture content in the heated mortar specimen accelerates carbonation and chloride penetration. The total pore volume and pore diameter also significantly affect their acceleration.

6) Although the residual compressive strength of the heated specimens is greater than 70% and CH is not dehydrated, the durability of heated specimens is degraded by heating.

Consequently, moisture at depths close to the exposed surface of mortar and concrete specimens during the heating is evaporated, and then, a part of vapor migrates to the inside and condenses into moisture inside the specimen. That phenomenon can be observed by the electrical resistivity method. It has shown that the electrical resistivity method, which is an in-situ resistance measurement and nondestructive method, can be carried out for post-fire concrete and mortar. The increase in pore volume caused by micro-crack and melting of PP fibers leads to easier penetration of CO_2 and chloride ions into the specimen after exposed to high temperature. Concrete with a low W/C has better strength and durability, but it develops more micro-cracks when exposed to high temperature. Although the addition of PP fibers is an effective method of preventing explosive spalling, PP fibers could contribute to degradation of durability of fire-exposed concrete.

8. Further research

It is well known that the high temperatures cause the movement of moisture inside the concrete, especially the region closest to the exposed surface. Although, the electrical resistivity method can be used to monitoring the behavior of moisture transportation, the method should be able to determine the exact internal relative humidity of concrete and mortar. The calibration specimens to determine the internal moisture movement were conducted, as seen in appendix, but the results are unclear. The calibration method should be developed to make more accuracy and improve more reliable. Then, the model to predict the moisture transportation inside heated specimen will be established with function of fire severity and type of concrete.

High temperature exposure resulting in concrete temperature up to 350° (at the exposed surface) reduces the strength but repairing to recover the load carrying capacity is commonly not necessary. However, this study shows that the liquid and gas transport properties are changed considerably due to the increment of pore and crack volume, regardless of the PP fibers. Thus, the resistance of frost damage should be investigated.

In this study, the concrete and mortar without any corrosion were used as specimen. Normally, the concrete structure in real life has been corroded by the environment, CO_2 from vehicle and chloride from sea, before fire accident occurring. Thus, the corroded concrete should be considered.

Generally, PP fiber is used for increasing pore volume of posed fire concrete and reducing spalling. But the PP fibers do not have a significant effect on the compressive strength and the increasement of pore volume reduces the compressive strength. Therefore, the idea is increasing pore volume of posed fire concrete to against spalling and keeping/increasing the compressive strength. The new material will be used for this idea such as ferronickel slag that it was used to increase the density and porosity of mortar without sacrificing compressive strength.

Finally, the damage of post-fire concrete depends on the fire severity. Therefore, the several of degree of fire damaged on concrete need to be studied further.

9. Acknowledgements

I would like to express my gratitude to my supervisor Professor Kenji Kawai for his kindness, valuable suggestions and giving me the opportunity to become a PhD-student and to Assistant Professor Yuko Ogawa and Dr.Phuong Trinh Bui for the valuable discussions during planning and test.

I would also like to thank Mr.Tatsuya Kitagawa for support during test.

Finally, I would also like to thank the Japan Concrete Institute (JCI) for fund, in part, of this research.

References

Anderberg, Y., (1997). "Spalling phenomena of HPC and OC." *International Workshop on Fire Performance of High-strength Concrete, National Institute of Standards and Technology (NIST)*, MD 13-14 February. NIST Special Publication 919, 69-73.

Annerel, E. and Taerwe, L., (2013). "Damage assessment of concrete structures exposed to fire." *Proceedings of the IABSE Conference Assessment, upgrading and refurbishment of infrastructures*, Rotterdam, Netherland, 6-8 May 2013, 1-8.

Architectural Institute of Japan (2015), "*Recommendations for Diagnosis and Repair Methods of Fire-damaged Buildings.*" Tokyo, Japan

Behnood, A. and Ghandehari, M., (2009). "Comparison of compressive and splitting tensile strength of high-strength concrete with and without polypropylene fibers heated to high temperatures." *Fire Safety Journal*, 44 (8), 1015-1022.

Bosnjak, J., Ozboth, J. and Hahn, R., (2013). "Permeability measurement on high strength concrete without and with polypropylene fibers at elevated temperatures using a new test set up." *Cement and Concrete Research*, 53, 104-111.

Bui, P. T., Ogawa, Y., Nakarai, K. and Kawai, K., (2016). "Electrical resistance measurement to assess moisture transfer in cement–based mortar through water absorbing and drying processes." *Proceedings of the Japan Concrete Institute (JCI)*, Fukuoka, Japan, 6-8 July 2016, 38, 813-818.

Chan, Y.N., Peng, G.F., and Anson, M., (1999). "Residual strength and pore structure of high strength concrete and normal strength concrete after exposure to high temperatures." *Cement and Concrete Composites,* 21(1), 23-27.

Chag, Y.F., Chen, Y.H., Sheu, M.S.and Yao, G.C. (2006) "Residual stress-strain relationship for concrete after exposure to high temperatures" *Cement and Concrete Research,* 36(10) 1999-2005.

Concrete Society (2008), "*Assessment, Design and Repair of Fire-damaged Concrete Structures.*" Technical Report No. 68, Camberley U.K.

Denoël, Ir.J.F., (2007). "*Fire Safety and Concrete Structures.*" Federation of Belgian Cement Industry, Belgiam.

Euro Code 2 (EC2) (2004). "*Design of Concrete Structures – part 1.2: general rues structural fire design",* European Committee for Standardization.

Elkey, W. and Sellevold, E.J., (1995). "*Electrical Resistivity of Concrete*", Oslo, Norwegian Road Research Laboratory.

Fujioka, S., Kawai, K., Nakarai, K. and Hayashi, A., (2013). "Measurement of moisture transfer using stainless steel in a water absorption process." *International Conference on Civil and Environmental Engineering (ICCEE)*, Dalian University of Technology, China, 24-25 September 2013, 222-224.

Georgali, B. and Tsakiridis, P.E., (2005). "Microsturcture of fire-damaged concrete. A case study." *Cement and concrete composites*, 27, 255-259.

Ghosh, S. and Nasser, K.W., (1996). "Effects of high temperature and pressure on strength and elasticity of lignite fly ash and silica fume concrete" *ACI Materials Journal*, 93(1), 51-60.

Hager, I., (2013). "Behavior of cement concrete at high temperature." *Bulletin of The Polish Academy of Sciences,* 61(1), 145-154.

Jansson, R., (2013). "*Fire spalling of concrete theoretical and experimental studies*." Thesis (PhD). KTH Stockholm, Sweden.

Joakim, A., (2015). "*Durability of fire exposed concrete.*" Thesis (PhD). Department of Civil and Architectural Engineering, KTH Royal Institute of Technology Stockholm, Sweden.

Kalifa, P., Chene, G. and Galle, C., (2001). "High-temperature behaviour of HPC with polypropylene fibres from spalling to microstructure." *Cement and Concrete Research*, 31 (10), 1487-1499.

Khoury, G.A., Willoughby, B., (2008). “Polypropylene fibres in heated concrete. Part 1: Molecular structure and materials behavior” *Magazine of Concrete Research,* 60 (2), 125-136.

Kodur, V., (2014). “Properties of Concrete at Elevated Temperatures.” *Civil Engineering,* 2014, 1-15.

Lin, W. M., Lin, T. D. and Powers-Couche, L.J., (1996). “Microstructures of fire-damaged concrete.” *ACI Materials Journal*, 93 (3), 199-205.

Lu, F., (2015). “*On the Prediction of Concrete spalling under fire*.” Thesis (PhD), ETH Zurich

Layssi, H., Ghods, P., Alizadeh, A.R. and Salehi, M., (2015). “Electrical Resistivity of Concrete.” *Concrete International*, 37 (5), 41-46.

Madhavi, T.Ch. and Annamalai, S., (2016). “Electrical Conductivity of Concrete.” *Journal of Engineering and Applied Sciences*, 11 (9), 5979-5982.

Mccarter, W.J., Emerson, M. and Ezirim, H., (1995). “Properties of concrete in the cove zone: developments in monitoring techniques.” *Magazine of Concrete Research*, 47, 243-251.

Mccarter, W.J., Watson, D.W. and Chrisp, T.M., (2001). “Surface Zone Concrete: Drying, Absorption, and Moisture Distribution.” *Journal of Materials in Civil Engineering*, 49-57.

Noumowe, A.N., Siddique, R. and Debicki, G., (2009). “Permeability of high-performance concrete subjected to elevated temperature (600 °C).” *Construction and Building Materials*, 23 (5), 1855-1861.

Omer, A., (2007). “Effects of elevated temperatures on properties of concrete.” *Fire Safety Journal*, 42 (8), 516-522.

Ozawa, M. and Morimoto, H., (2014). “Effects of various fibres on high-temperature spalling in high-performance concrete.” *Construction and Building Materials*, 71, 83-92.

Papayianni, J. and Valiasis, T., (1991). “Residual mechanical properties of heated concrete incorporating different pozzolanic materials.” *Materials and Structures,* 24, 115-121

Poon, C. S., Azhar, S., Anson, M. and Wong, Y.L., (2001). “Comparison of the strength and durability performance of normal and high-strength pozzolanic concretes at elevated temperatures.” *Cement & Concrete Research*, 31 (9), 1291-1300.

Poon, C. S., Azhar, S., Anson, M. and Wong, Y.L., (2003). “Performance of metakaolin concrete at elevated temperatures.” *Cement & Concrete Composites*, 25 (1), 83-89.

Rajabipour, F., Weiss, W.J., and Abraham, D. (2004). “Insitu Electrical Conductivity Measurements to Assess Moisture and Ionic Transport in Concrete.” *Proceedings of the International RILEM Symposium,* Evanston, Illinois.

Richardson, A. and Dave, U.V., (2008). “The effect of polypropylene fibres within concrete with regard to fire performance in structures” *Structural Survey*, 26(5), 435-444

Rongviriyapanich, R., Sato, Y. and Pansuk, W., (2016). “Damage evaluations of oven-dried mortar subjected to one-directional fire.” *Journal of ACF*, 2 (1), 31-45.

Schneider, U. and Horvath, J. (2003). “Behavior of Ordinary Concrete at High Temperatures” *Research reports of Vienna University of Technology*, Vienna.

Serrano, R., Cobo, A., Priet, M.I. and Gonzalez, M.N., (2016). “Analysis of fire resistance of concrete with polypropylene or steel fibers.” *Construction and Building Materials*, 122, 302-309.

The International Federation for Structural Concrete (fib) (2008), “*Fire design of concrete structures-structural behaviour and assessment.*” Bulletin 46, Switzerland

The International Federation for Structural Concrete (fib) (2007), “*Fire design of concrete structures-structural materials, structures and modelling.*” Bulletin 38, Switzerland

Wade, C.A., Gerlich, J.T. and Abu, A., (2014), “The Relationship Between Fire Severity and Time-Equivalence.” Study report, BRANZE from the Building Research Levy.

Yermak, N., Pliya, P., Beaucour, A.-L., Simon, A. and Noumowe, A., (2017) “Influence of steel and/or polypropylene fibres on the behaviour of concrete at high temperature:

Spalling, transfer and mechanical properties." *Construction and Building Materials,* 132, 240-250.

Yufang, F., Lianchong, Li., (2011) "Study on mechanism of thermal spalling in concrete exposed to elevated temperatures." *Materials and Structures*, 44, 361-376.

Zdenek, P., (1997) "Analysis of pore pressure, thermal stress and fracture in rapidly heated concrete." *International Workshop on Fire Performance of High–strength Concrete, National Institute of Standards and Technology (NIST)*, MD 13-14 February, NIST Special Publication 919, 155-164.

Zhang, P. and Li, Q., (2013). "Effect of polypropylene fiber on durability of concrete composite containing fly ash and silica fume." *Composites: Part B*, 45 (1), 1587-1594.

Appendix

Determination of internal relative humidity and relative water content

For calibration specimen, the mortar specimen of 40-mm width, 40-mm height and 15-mm depth with stainless steel rod was cut from the heated and unheated prismatic mortar and concrete specimens. For concrete specimen, the calibration specimens were also cut from heated and unheated specimens into dimension of 100-mm width, 100- height and 15 mm depth with stainless steel rod. The calibration specimens were exposed to different humidity boxes at 20 °C and measured the electrical resistivity in order to obtain the relationship between internal relative humidity and electrical resistivity, assuming that the relative humidity in the specimens reaches the same humidity as a state of equilibrium in the box. The creation of specified humidity conditions in the box that the calibration specimens absorb or desorb moisture until the mass of specimen became constant were made using saturated salt solutions as shown in Table 11. Then, the equilibrium relative humidity was obtained.

Table 11 The saturated salt solution

Relative humidity (%)	Saturated salt solution
98	Potassium sulfate
85	Potassium chloride
75	Sodium chloride
70	Potassium iodide
60	Sodium bromide
43	Potassium carbonate
33	Magnesium chloride
23	Potassium acetate
12	Lithium chloride
6	Lithium bromide

Resistivity and relative water content of calibration specimens

The relation between resistivity and relative water content of calibration mortar specimens

The electrical resistance of calibration specimens was calculated in term of electrical resistivity. The correlation between resistivity and relative water content of calibration specimens at each depth of specimens are shown in Fig. 34. It could be explained that the electrical resistivity of calibration specimens increased with the decrease in internal relative humidity at 20°C. By the correlation between the electrical resistivity and internal relative humidity of calibration specimens, the equations were obtained in order to determine the internal relative humidity of mortar specimens and are also shown in Table 12. R-squared values of equations vary from approximate 0.3 to 0.65.

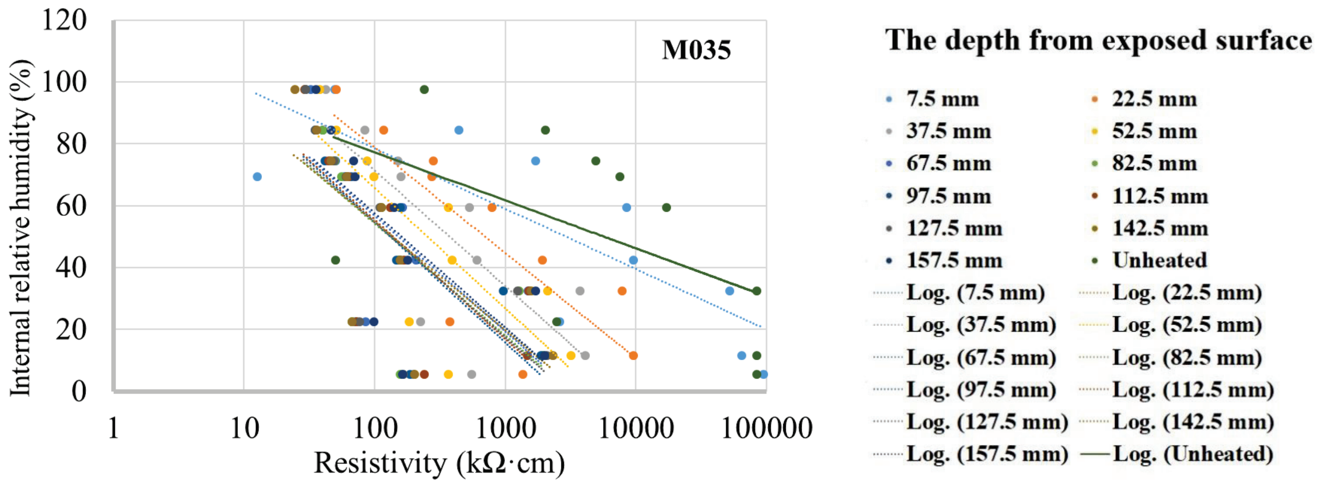

a) Influence of internal relative humidity on resistivity of calibration specimens of the M035

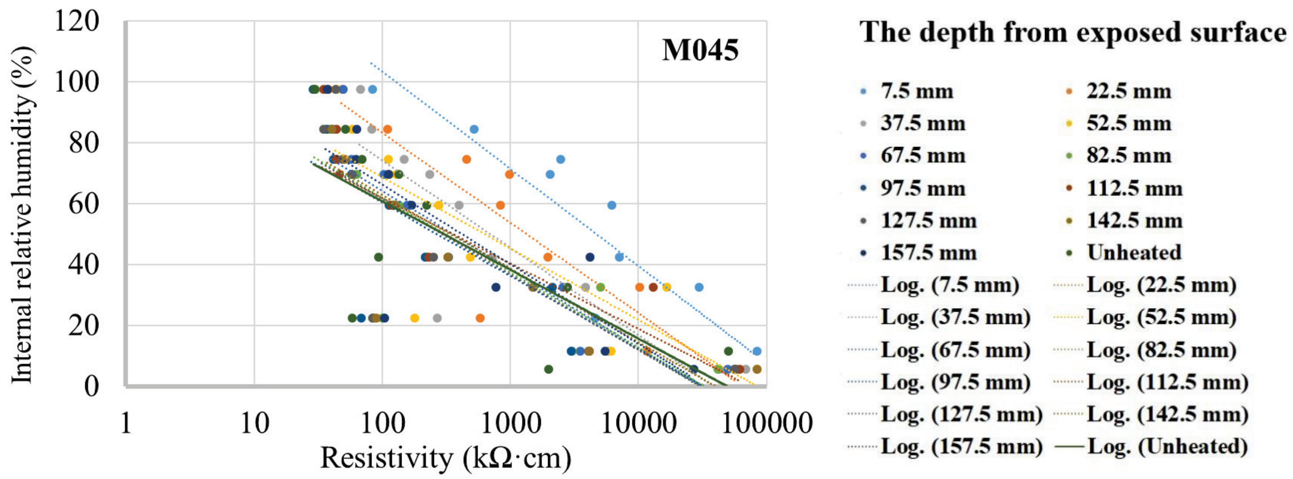

b) Influence of internal relative humidity on resistivity of calibration specimens of the M045

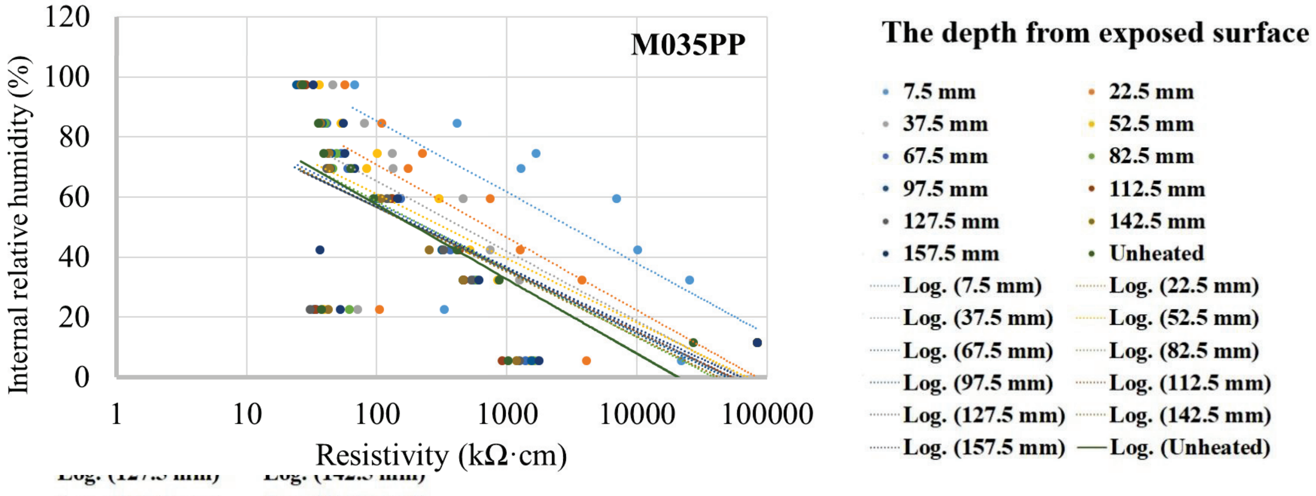

c) Influence of internal relative humidity on resistivity of calibration specimens of the M035PP

Fig. 34 Influence of internal relative humidity on resistivity of calibration specimens of the M035, M045 and M035PP specimens

Table 12 The equations of internal relative humidity on resistivity of the mortar calibration specimens

Distance from exposed surface (mm)	M035 (eq)(R^2)	M045 (eq)	M035PP (eq)
7.5	H=-8.86ln(ρ)+119.9 (13)	H=-12.78ln(ρ)+159.44 (25)	H=-9.324ln(ρ)+125.65 (37)
22.5	H=-10.1ln(ρ)+118.39 (14)	H=-13.53ln(ρ)+146.78 (26)	H=-10.47ln(ρ)+118.98 (38)
37.5	H=-15.98ln(ρ)+145.23 (15)	H=-12.14ln(ρ)+130.15 (27)	H=-10.05ln(ρ)+111.67 (39)
52.5	H=-16.95ln(ρ)+144.26 (16)	H=-8.79ln(ρ)+108.37 (28)	H=-9.27ln(ρ)+103.64 (40)
67.5	H=-15.2ln(ρ)+127.01 (17)	H=-10.28ln(ρ)+110.49 (29)	H=-9.19ln(ρ)+100.62 (41)
82.5	H=-15.04ln(ρ)+123.09 (18)	H=-10.82ln(ρ)+111.98 (30)	H=-9.8ln(ρ)+104.1 (42)
97.5	H=-15.86ln(ρ)+128.38 (19)	H=-10.52ln(ρ)+109.38 (31)	H=-9.14ln(ρ)+99.19 (43)
112.5	H=-15.7ln(ρ)+128.52 (20)	H=-9.86ln(ρ)+107.58 (32)	H=-9.05ln(ρ)+98.76 (44)
127.5	H=-15.16ln(ρ)+125.02 (21)	H=-10.22ln(ρ)+109.06 (33)	H=-9.03ln(ρ)+98.62 (45)
142.5	H=-14.68ln(ρ)+123.46 (22)	H=-10.47ln(ρ)+111.35 (34)	H=-9.35ln(ρ)+100.29 (46)
157.5	H=-15.42ln(ρ)+129.14 (23)	H=-11ln(ρ)+117.34 (35)	H=-9.72ln(ρ)+104.99 (47)
Unheated specimen	H=-13.48ln(ρ)+164.48 (24)	H=-9.54ln(ρ)+107.75 (36)	H=-9.15ln(ρ)+100.16 (48)

* ρ = electrical resistivity

The relation between resistivity and relative water content of calibration concrete specimens

Similar to mortar specimens, the correlations between the electrical resistivity and relative water content of concrete calibration specimens at the depths 7.5, 27.5, 47.5, 67.5, 87.5 and 147.5 mm from exposed surface were shown in Fig. 35. The equations to determine the internal relative humidity of concrete specimens were shown in Table 13. R-squared values of equations vary from 0.60 to 0.75.

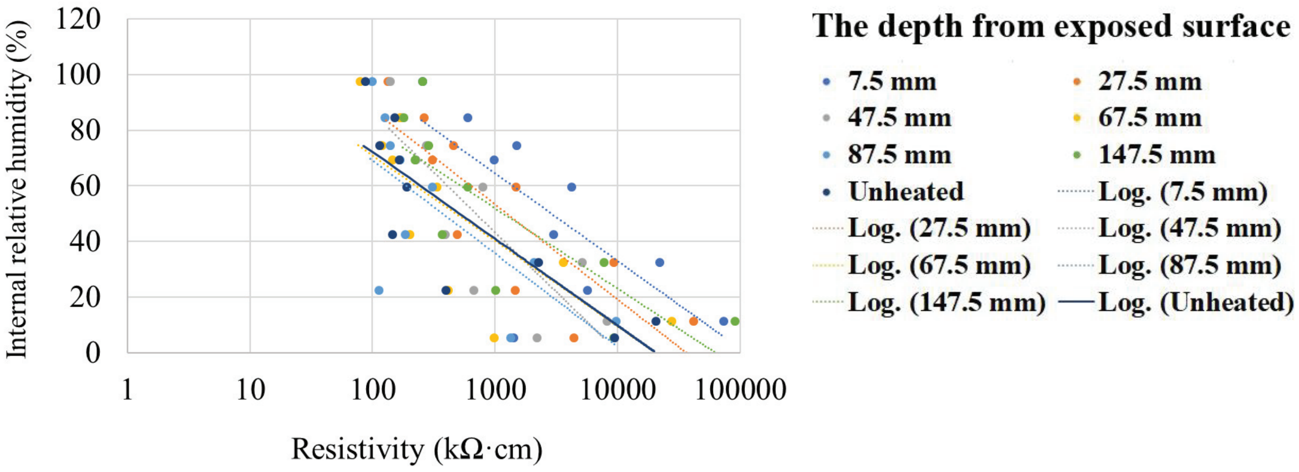

a) Influence of internal relative humidity on resistivity of calibration specimens of the C035

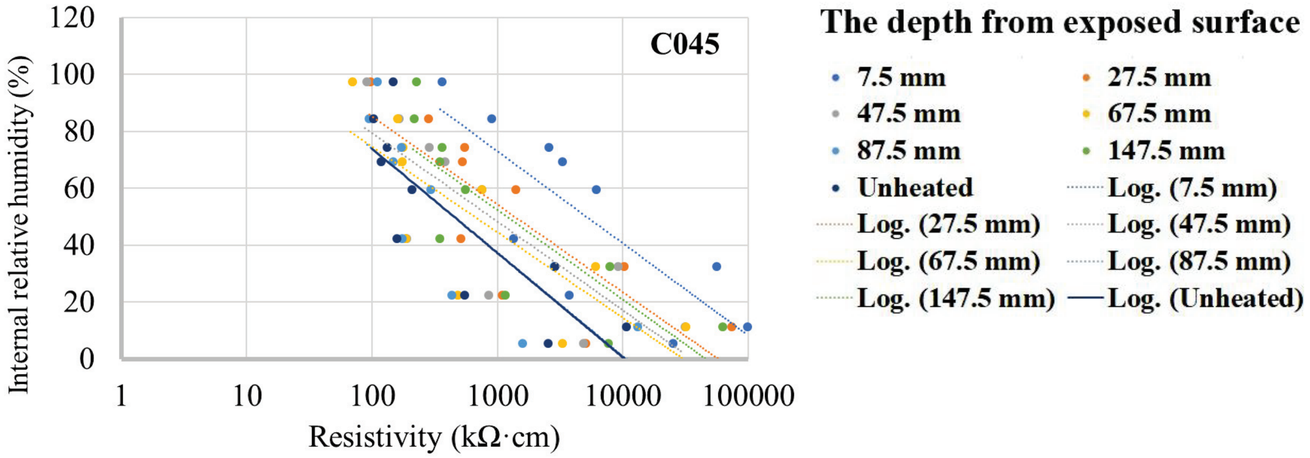

b) Influence of internal relative humidity on resistivity of calibration specimens of the C045

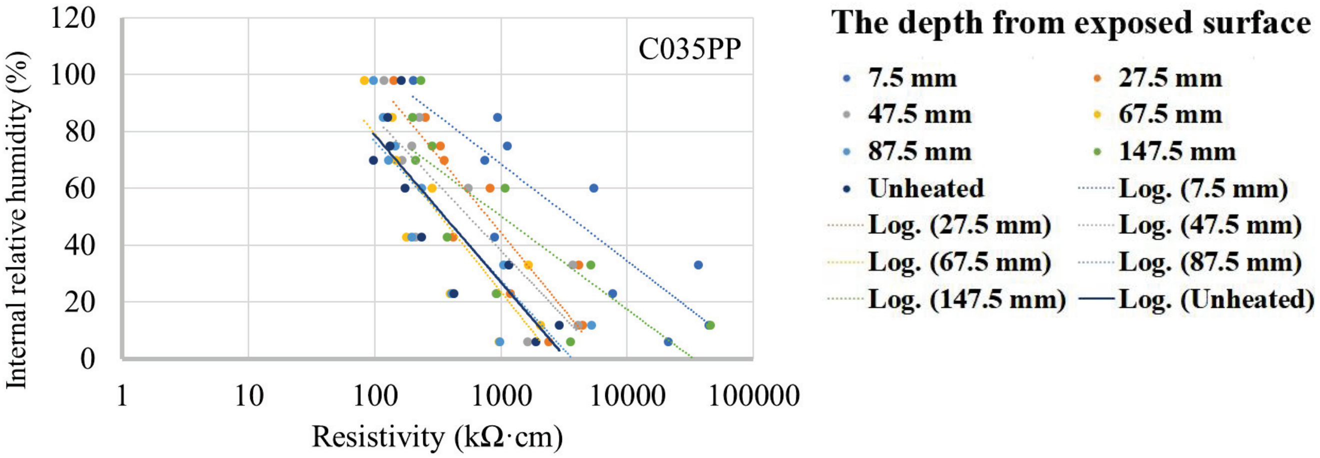

c) Influence of internal relative humidity on resistivity of calibration specimens of the C035PP

Fig. 35 Influence of internal relative humidity on resistivity of calibration specimens of the C035, C045 and C035PP specimens

Table 13 The equations of internal relative humidity on resistivity of the concrete calibration specimens

Distance from exposed surface (mm)	C035 (eq)	C045 (eq)	C035PP (eq)
7.5	H=-13.66ln(ρ)+158.91(49)	H=-14.05ln(ρ)+170.11 (56)	H=-14.81ln(ρ)+170.88 (63)
27.5	H=-14.83ln(ρ)+155.84 (50)	H=-13.53ln(ρ)+146.78 (57)	H=-23.49ln(ρ)+206.64 (64)
47.5	H=-18.65ln(ρ)+172.2 (51)	H=-13.52ln(ρ)+141.75 (58)	H=-20.34ln(ρ)+178.56 (65)
67.5	H=-13.33ln(ρ)+132.39 (52)	H=-13.04ln(ρ)+134.69 (59)	H=-24.17ln(ρ)+190.55 (66)
87.5	H=-14.56ln(ρ)+136.29 (53)	H=-15.82ln(ρ)+146.69 (60)	H=-21.25ln(ρ)+174.49 (67)
147.5	H=-12.53ln(ρ)+138.55 (54)	H=-14.05ln(ρ)+170.11 (61)	H=-14.28ln(ρ)+148.95 (68)
Unheated specimen	H=-13.54ln(ρ)+134.56 (55)	H=-15.91ln(ρ)+147.21 (62)	H=-22.49ln(ρ)+182.37 (69)

*ρ = electrical resistivity

Internal relative humidity

Mortar specimens

Using equations (13) – (48), internal relative humidity of M035, M045 and M035PP specimens are shown in Fig. 36. It appears that the internal relative humidity of M045 and M035PP of the unheated specimens are approximately 65% at the ages of 58 days, which is nearly to 60%RH of storing place. Meanwhile, the internal relative humidity of M035 unheated specimen is over 100%. The internal relative humidity of all unheated specimens constantly increased after heating time (i.e., the ages of 58, 118, and 178 days). After heating, there appeared that the moisture of M045 and M035PP specimen at the depths of 7.5 and 22.5 mm from the exposed surface suddenly decreased by approximately 30%, compared with unheated specimen. Meanwhile, the internal relative humidity at the other depth increased. Then, the internal relative humidity of heated specimen at the depth of 7.5 and 22.5 mm slightly decreased in the greater time, while the other depths were slightly increasing. The tendency of decreasing also occurred on the unheated specimen.

However, for the specimen with W/C of 0.35 without PP fibers, the moisture of unheated specimens was over 100% which the moisture might be not correspond with electrical resistivity. The reason for this phenomenon is still not know.

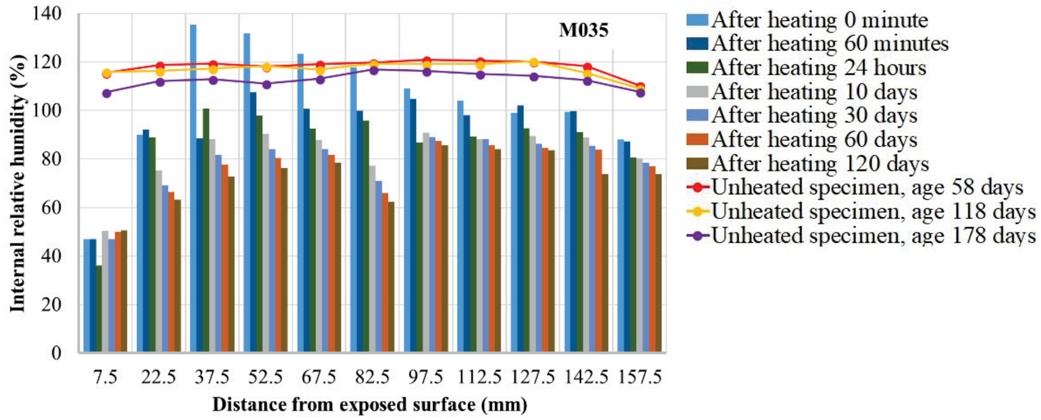

a) Moisture transfer of M035 specimen

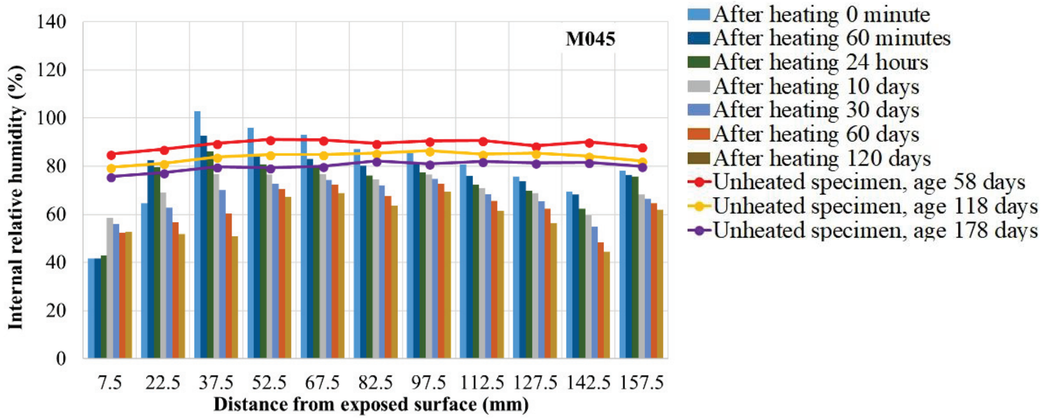

b) Moisture transfer of M045 specimen

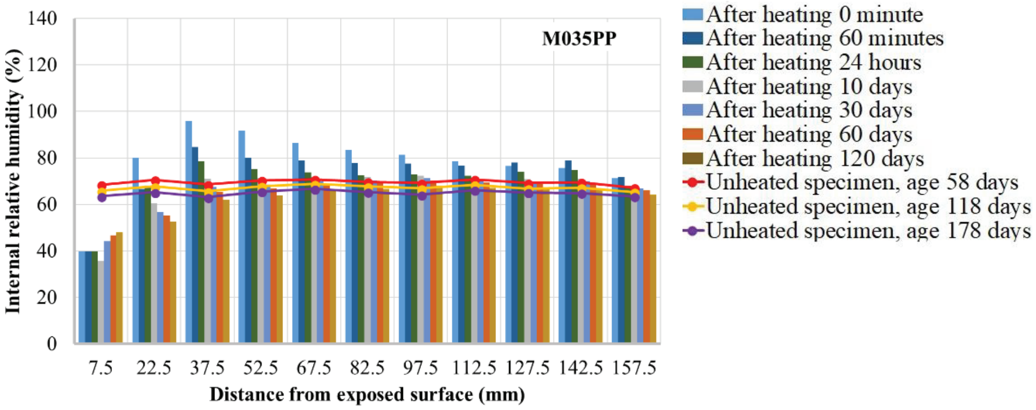

c) Moisture transfer in M035PP specimen

Fig. 36 Moisture transfer in M035, M045 and M035PP specimens

Concrete specimens

Similar to mortar specimen, the equations 49-69 were used to determine the internal relative humidity of the concrete specimens before and after heating. As seen in Fig. 37, the internal relative humidity of unheated concrete specimens is approximately 100% at the ages of 58 days, while C035PP specimen reached to approximate 120%. They could be observed that the internal relative humidity at any position of unheated specimens was quite constant at each age. Then, the internal relative humidity of all unheated concrete specimens constantly decreased in the greater time (i.e., the ages of 118 and 178 days).

After heating, the internal relative humidity at a depth 7.5 mm from exposed surface of C035, C045 and C035PP suddenly decreased to approximate 30, 45 and 70% after removing from the hot plate, respectively. Meanwhile, they suddenly increased in the greater depth of all heated specimens which are over 100% and internal relative humidity of unheated specimens. After that, the internal relative humidity at the greater depth continuously decreased until 120 days after heating. However, at 30 days after heating, there was observed that the internal relative humidity of all heated specimens was lower than that the unheated specimen at the same ages. There were also observed at 120 days after heating.

It appears that the internal relative humidity of M045 and M035PP of unheated specimens are approximately 65% at the ages of 58 days, which is nearly to 60%RH of storing place. Meanwhile, the internal relative humidity of M035 unheated specimen is over 100%. The internal relative humidity of all unheated specimens constantly increased after heating time (i.e., the ages of 58, 118, and 178 days). After heating, there appeared that the moisture of M045 and M035PP specimen at the depths of 7.5 and 22.5 mm from the exposed surface suddenly decreased by approximately 30%, compared with unheated specimen, after removing from the hot plate. Meanwhile, the internal relative humidity at the other depth increased as seen in Fig. 37. After storing, the internal relative humidity of heated specimen at the depth of 7.5 and 22.5 mm slightly decreased in the greater time, while the other depths were slightly increasing. The tendency of decreasing also occurred on the unheated specimen.

However, for the specimen with W/C of 0.35 without PP fibers, the moisture of unheated specimens was over 100% which the moisture might be not correspond with electrical resistivity. The reason for this phenomenon is still not know.

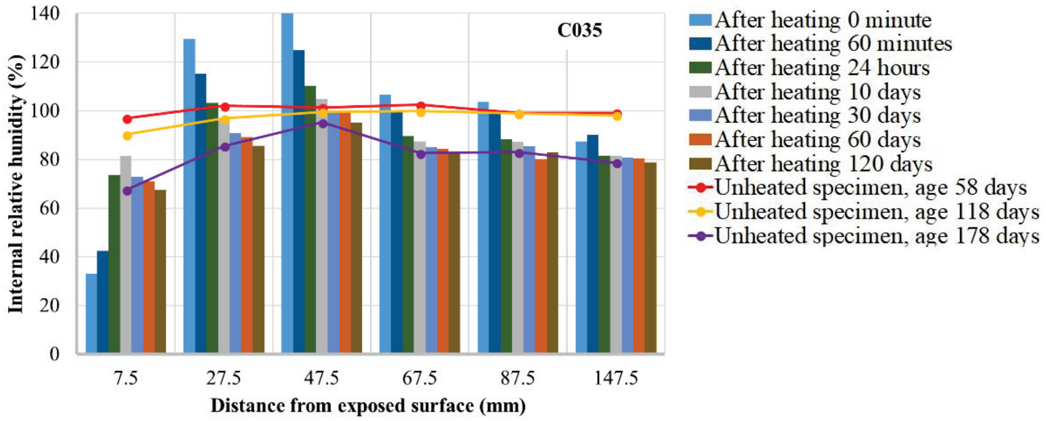

a) Moisture transfer in C035 specimen

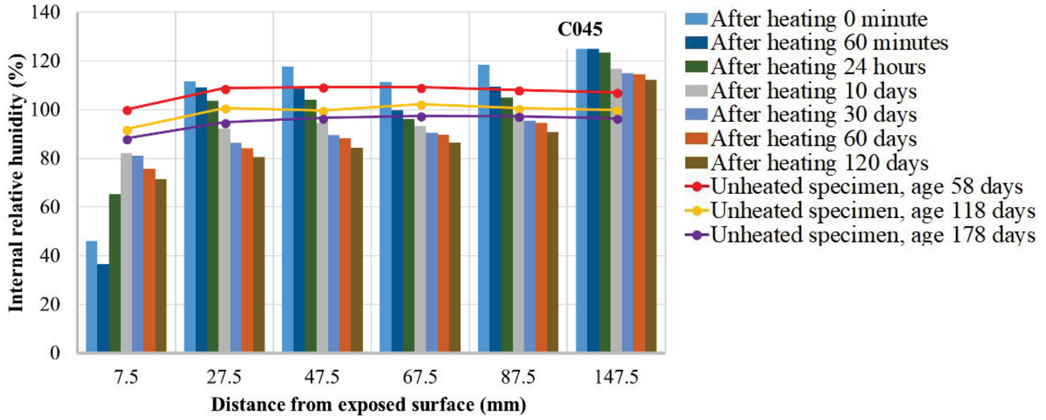

b) Moisture transfer in C045 specimen

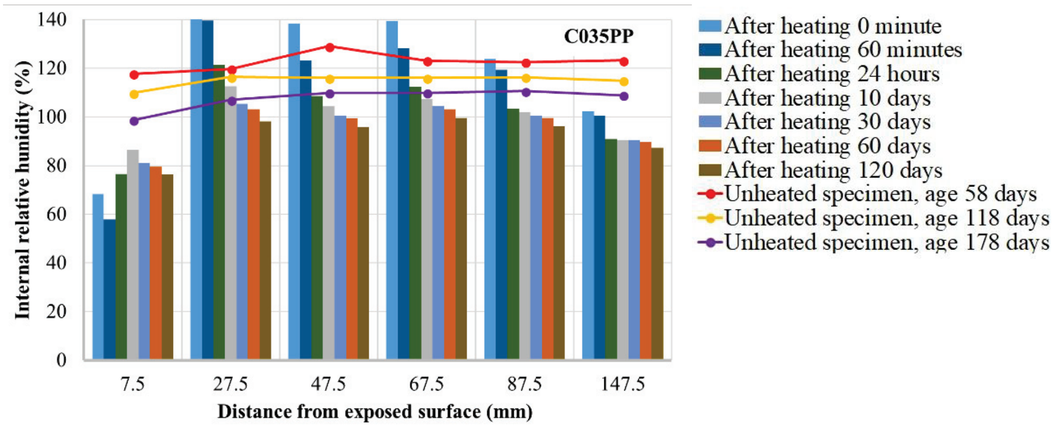

c) Moisture transfer in C035PP

Fig. 37 Moisture transfer in C035, C045 and C035PP specimens

Image of carbonation depth

Mortar with W/C of 0.35

Time (week)	Photo	
	Heated	Unheated
0	-	-
1		
4		
8		
13		
26		

Mortar with W/C of 0.45

Time (week)	Photo	
	Heated	Unheated
0		
1	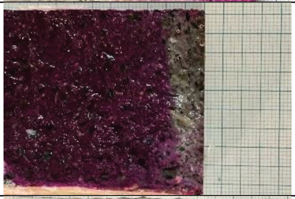	
4	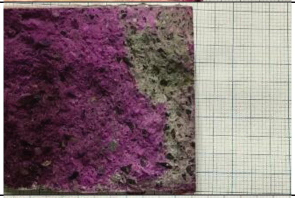	
8		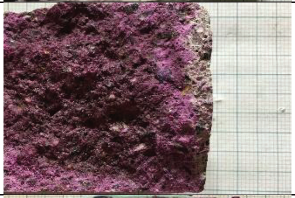
13		
26		

Mortar with W/C of 0.35 with PP fibers

Time (week)	Photo	
	Heated	Unheated
0		
1	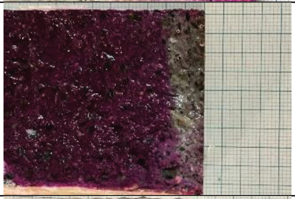	
4	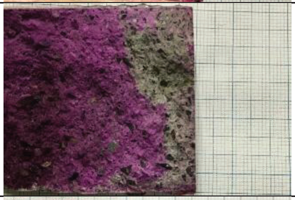	
8		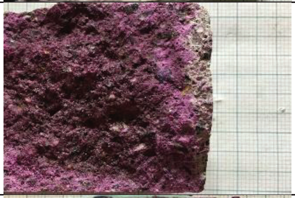
13		
26		

Concrete with W/C of 0.35

Time (week)	Photo	
	Heated	Unheated
0		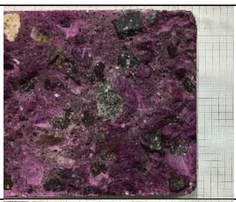
1	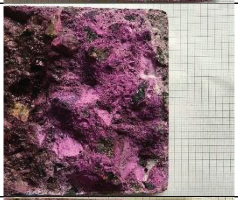	
4	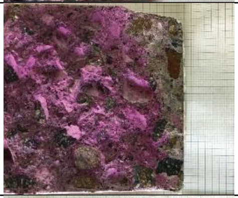	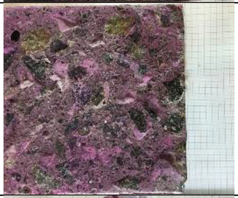
8		
13		
26	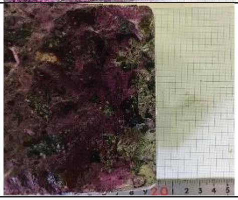	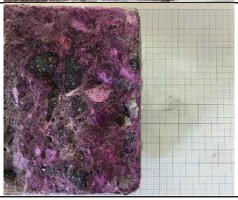

Concrete with W/C of 0.45

Time (week)	Photo	
	Heated	Unheated
0		
1	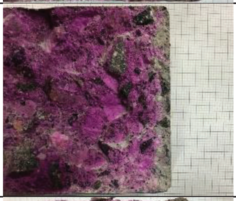	
4		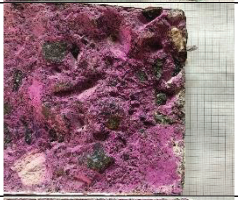
8	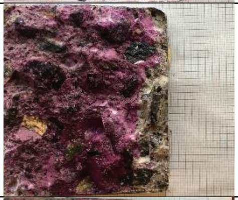	
13		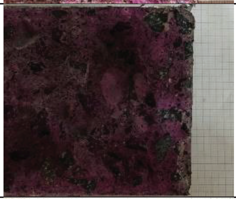
26		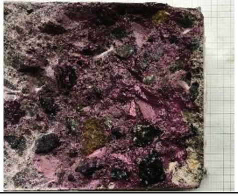

Concrete with W/C of 0.35 with PP fiber

Time (week)	Photo	
	Heated	Unheated
0	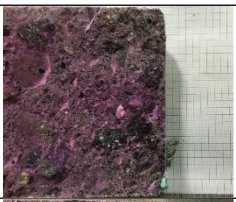	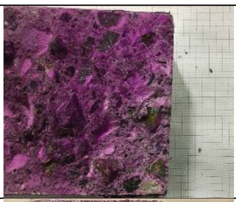
1	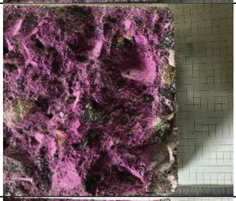	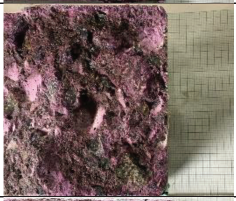
4		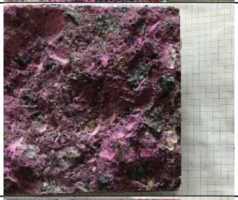
8		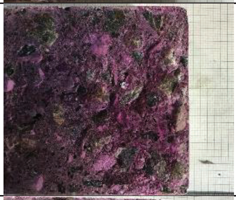
13	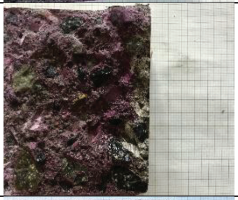	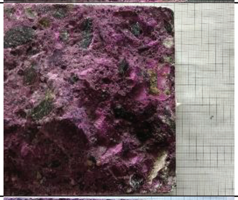
26		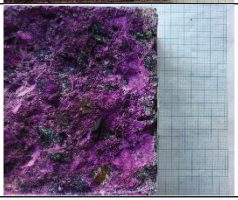

Image of chloride penetration depth

Mortar with W/C of 0.35

Wet-dry cycle (cycle)	Penetration depth	
	Heated	Unheated
15	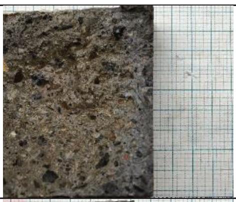	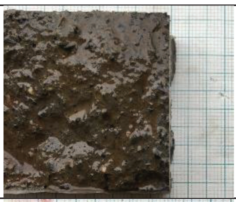
30	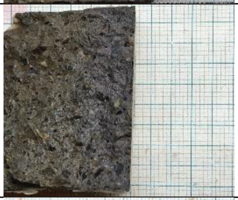	
45		

Mortar with W/C of 0.45

Wet-dry cycle (cycle)	Penetration depth	
	Heated	Unheated
15	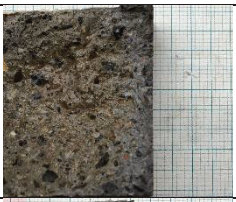	
30		
45		

Mortar with W/C of 0.35 with PP fibers

Wet-dry cycle (cycle)	Penetration depth	
	Heated	Unheated
15	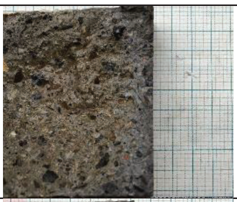	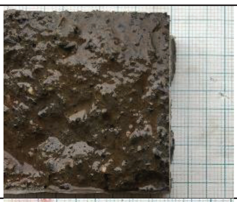
30	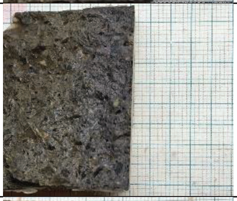	
45		

Concrete with W/C of 0.35

Wet-dry cycle (cycle)	Penetration depth	
	Heated	Unheated
15		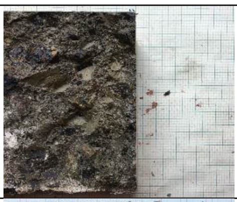
30	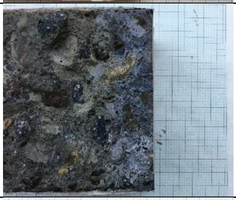	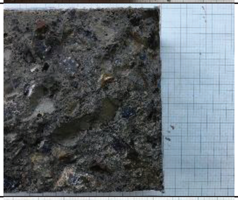
45		

Concrete with W/C of 0.45

Wet-dry cycle (cycle)	Penetration depth	
	Heated	Unheated
15	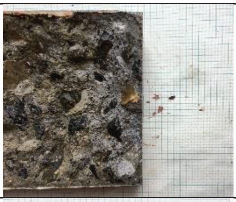	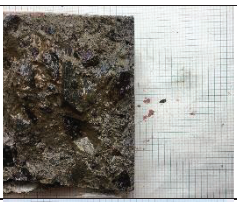
30	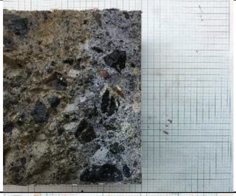	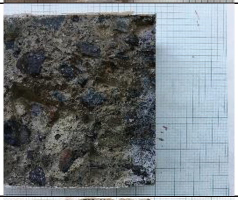
45	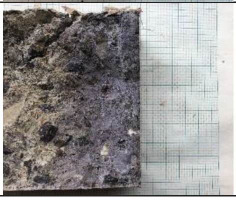	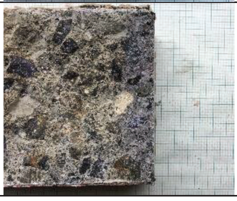

Concrete with W/C of 0.35 with PP fibers

Wet-dry cycle (cycle)	Penetration depth	
	Heated	Unheated
15	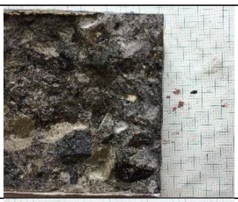	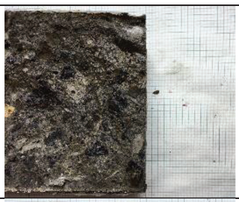
30	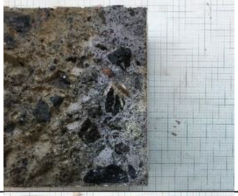	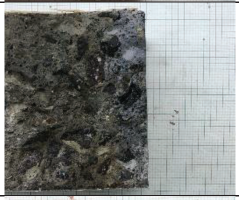
45